UNIVERSIDAD DE LA REPÚBLICA

PLAN DE ESTUDIOS MAESTRÍA Y DOCTORADO EN INGENIERÍA MECÁNICA

FACULTAD DE INGENIERÍA

Dinámica de fluidos reactivos computacional

Unidad 5. Aplicaciones de ingeniería

Prof. Leonel R Cancino, Dr. Eng.
leonel.cancino@labmci.ufsc.br

Unidad 5. Aplicaciones de ingeniería

5.1 Introducción

5.2 Llamas piloto (metano, acetileno, butano)

5.3 Quemadores tipo flauta

5.4 Simulación de un horno residencial

5.5 Complejidad numérica y fenológica de la combustión en un motor de combustión interna

Introducción

Development of combustion chambers with flute-burners in residential ovens.

Llamas piloto (metano, acetileno, butano)

Laminar 3D flame of methane.

without *buoyancy effects.*

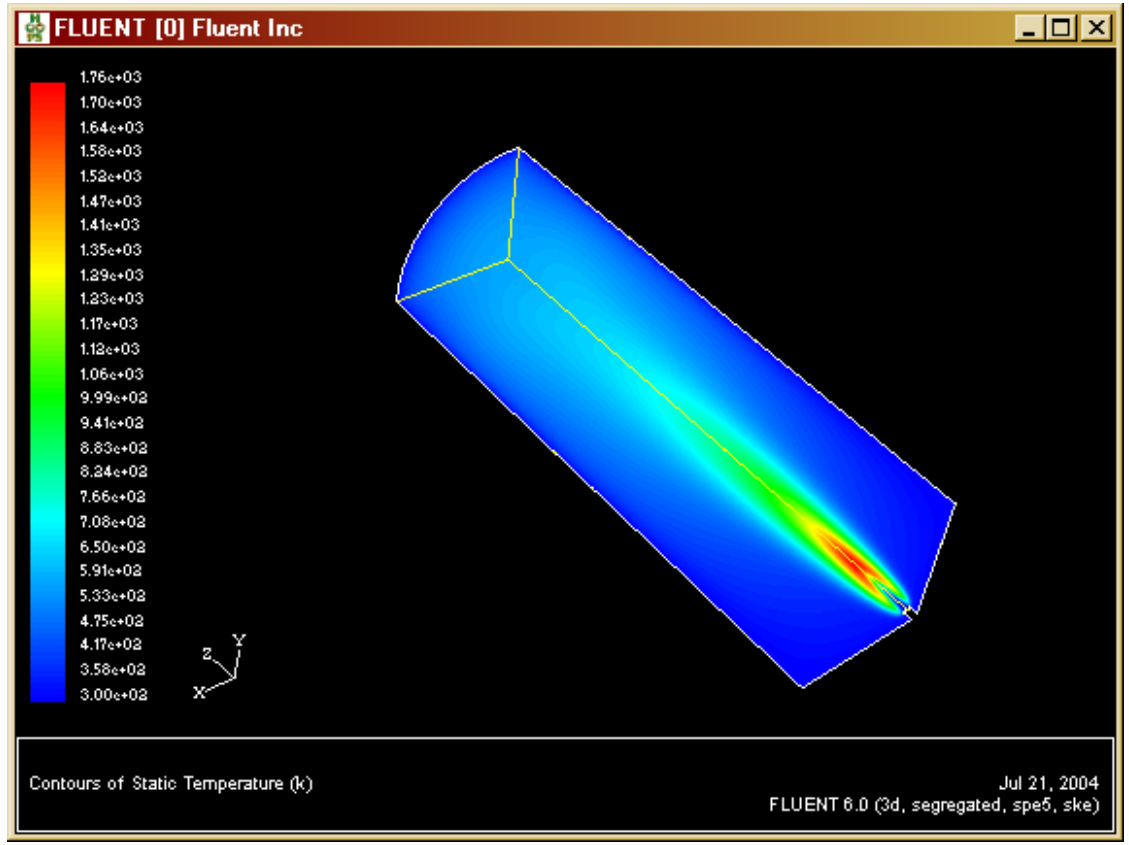

with *buoyancy effects.*

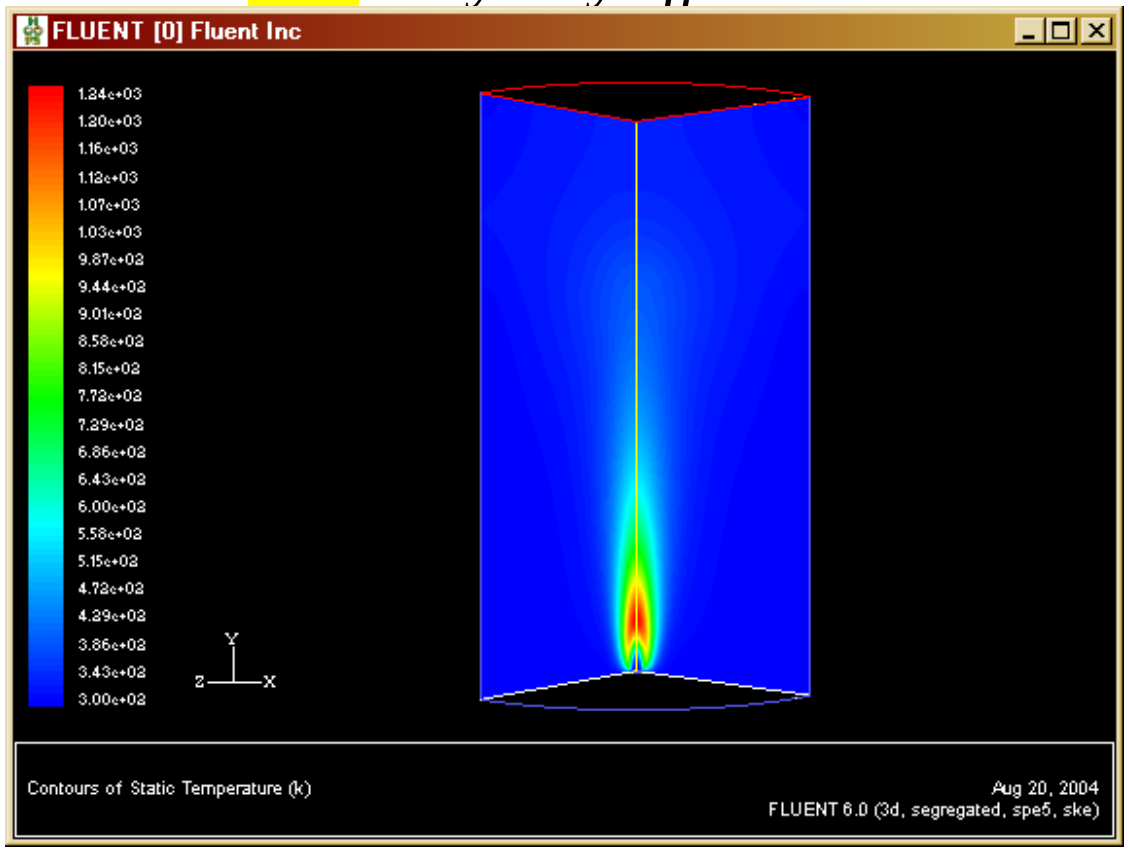

Llamas piloto (metano, acetileno, butano)

Laminar 3D flame of methane.

without *buoyancy effects.*

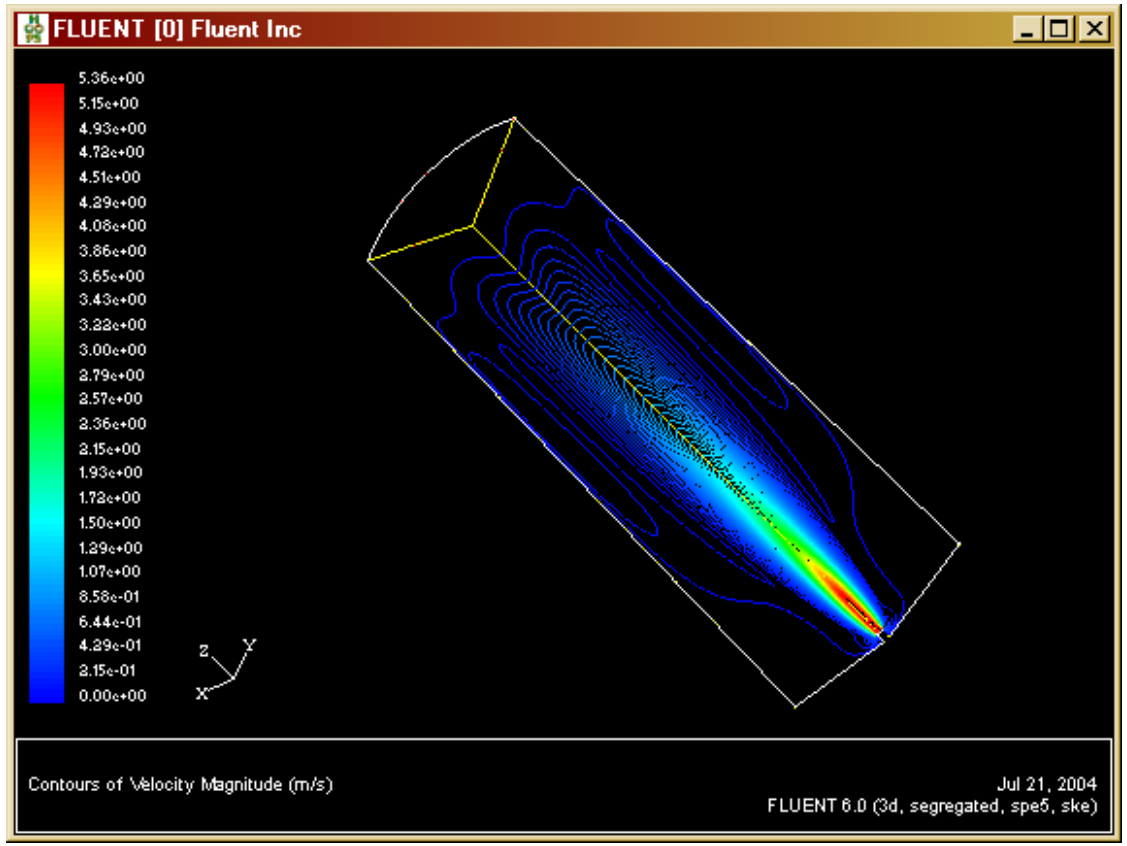

with *buoyancy effects.*

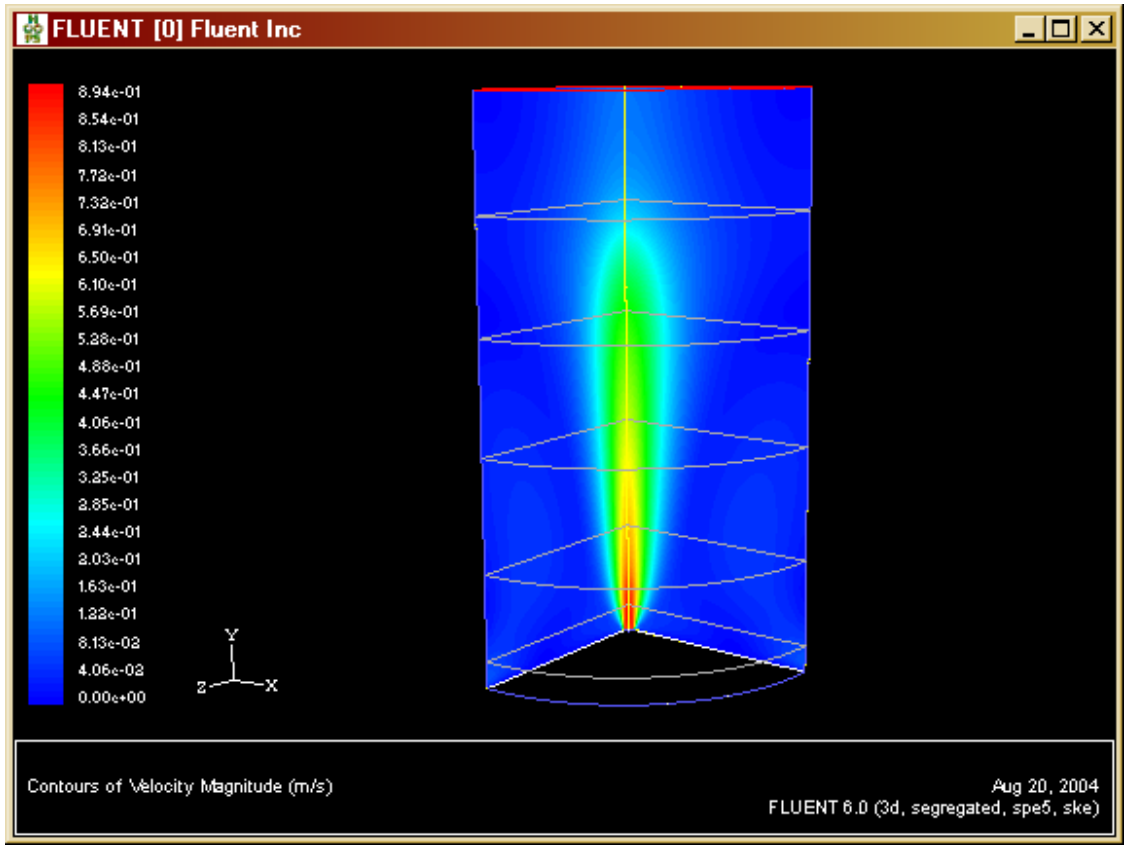

Llamas piloto (metano, acetileno, butano)

Laminar 3D flame of methane.

without buoyancy effects.

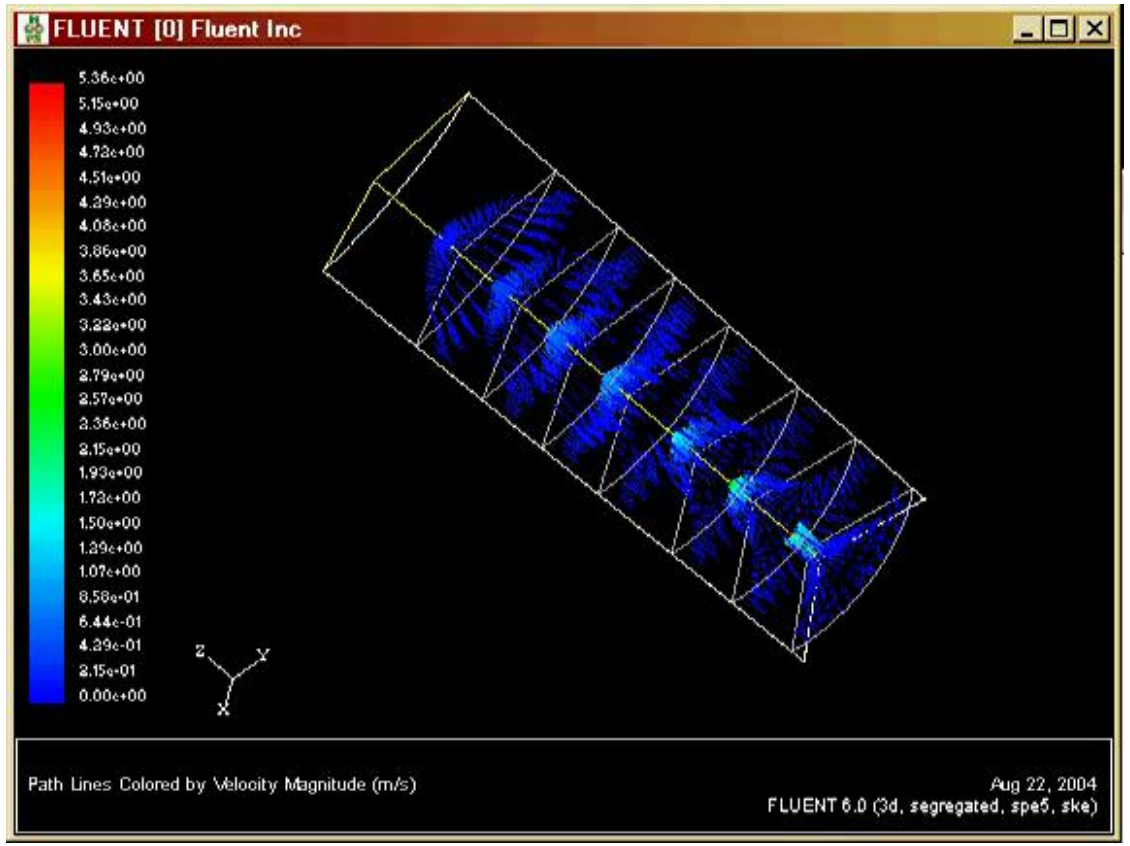

with buoyancy effects.

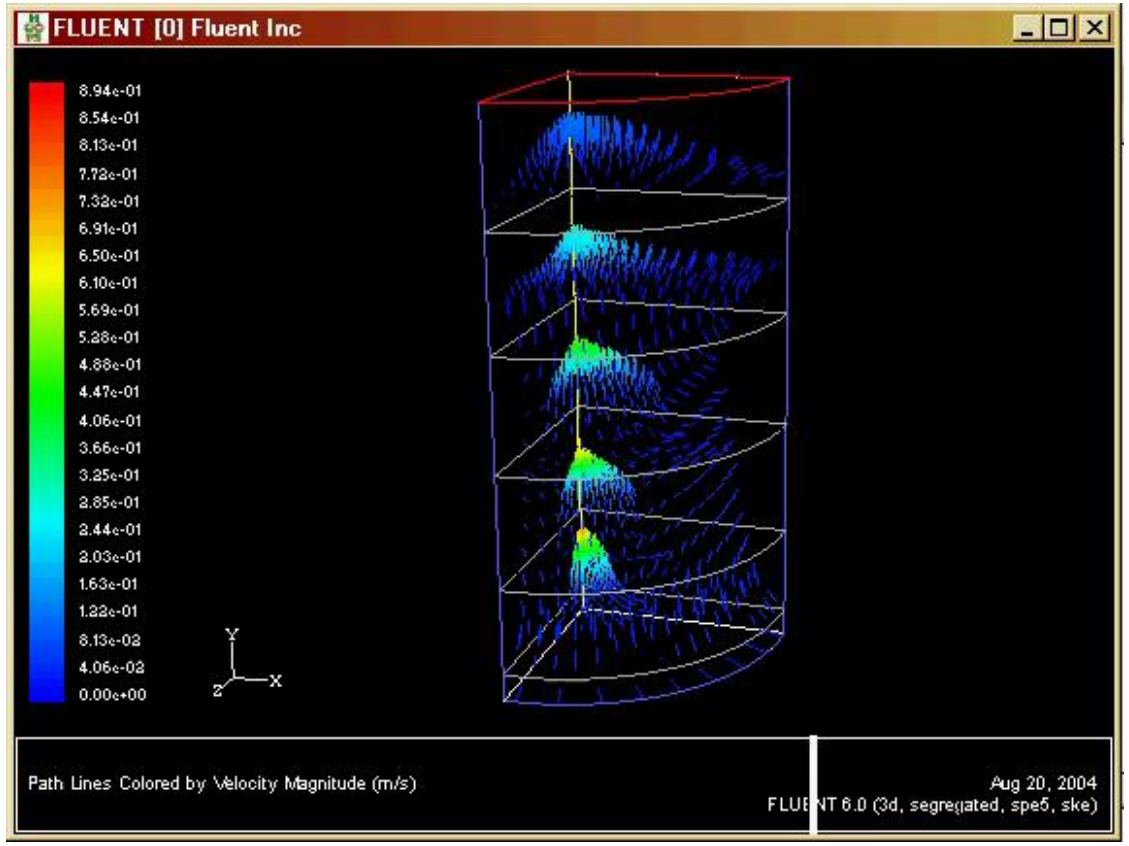

Quemadores tipo flauta

Development of combustion chambers with flute-burners in residential ovens.

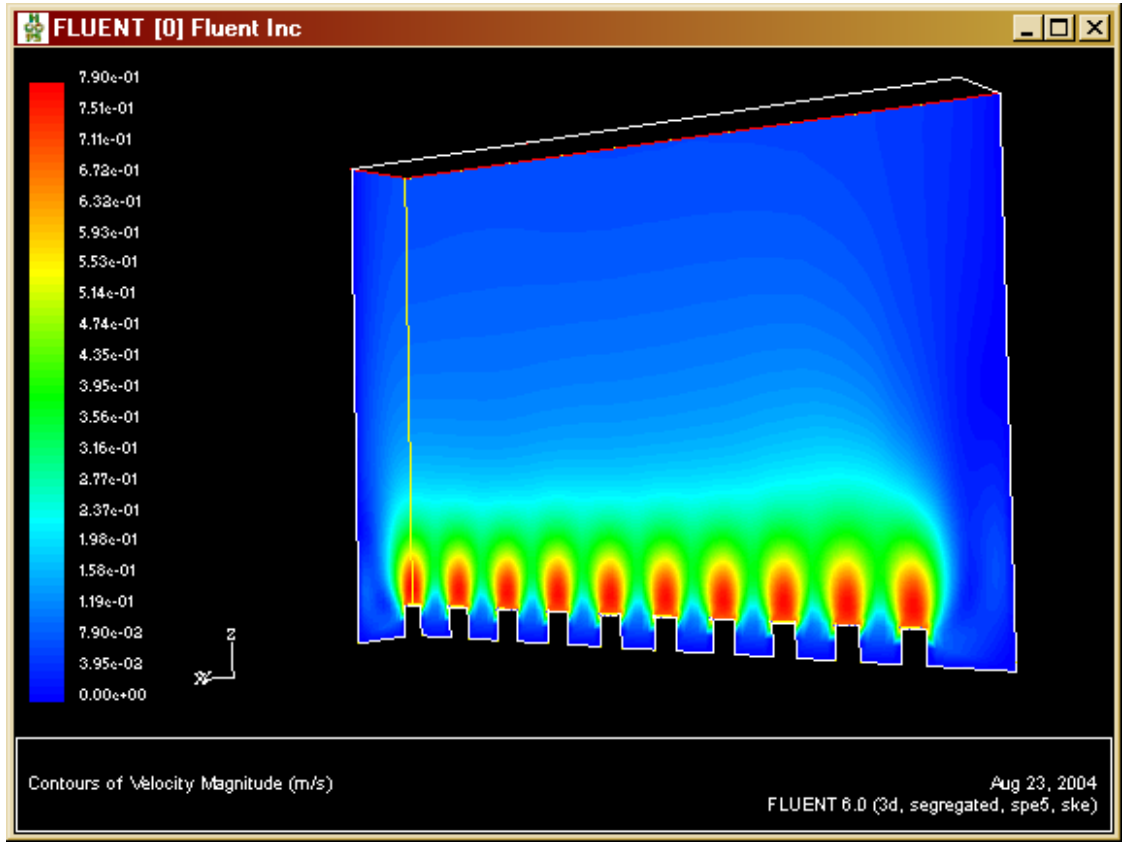

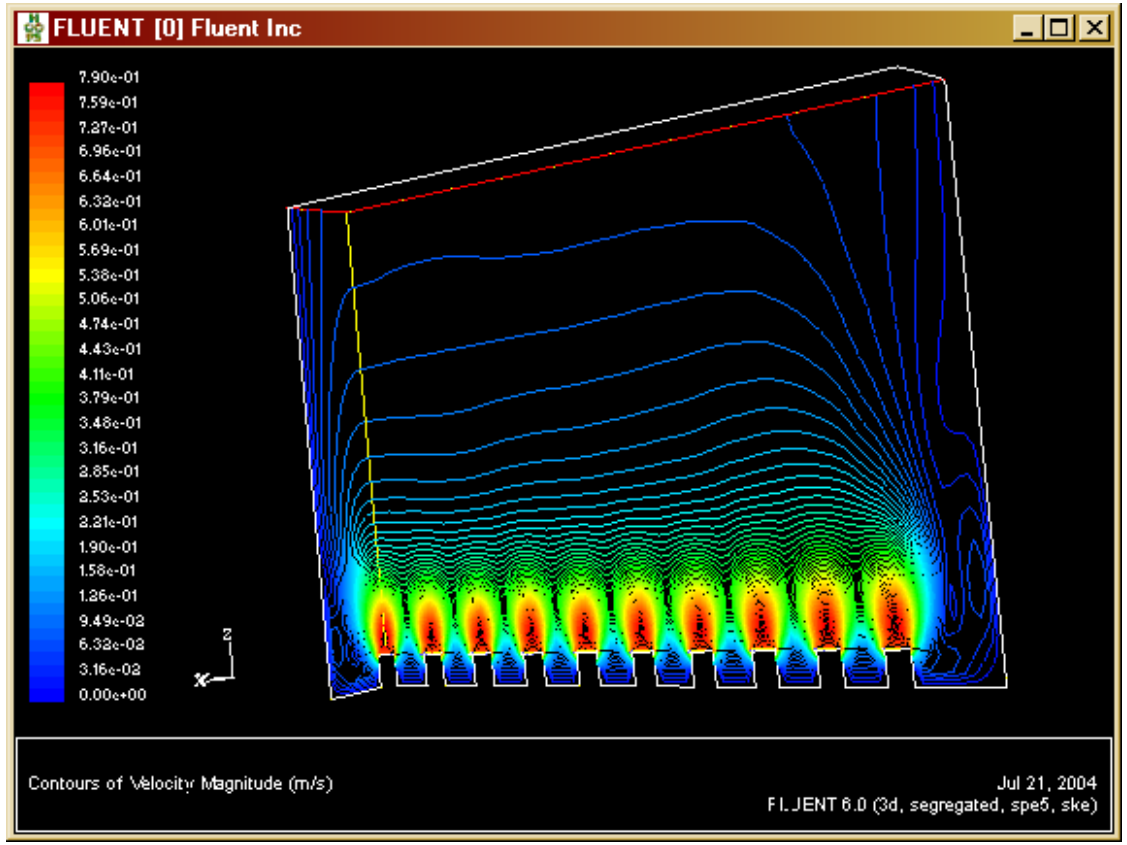

Quemadores tipo flauta

Development of combustion chambers with flute-burners in residential ovens.

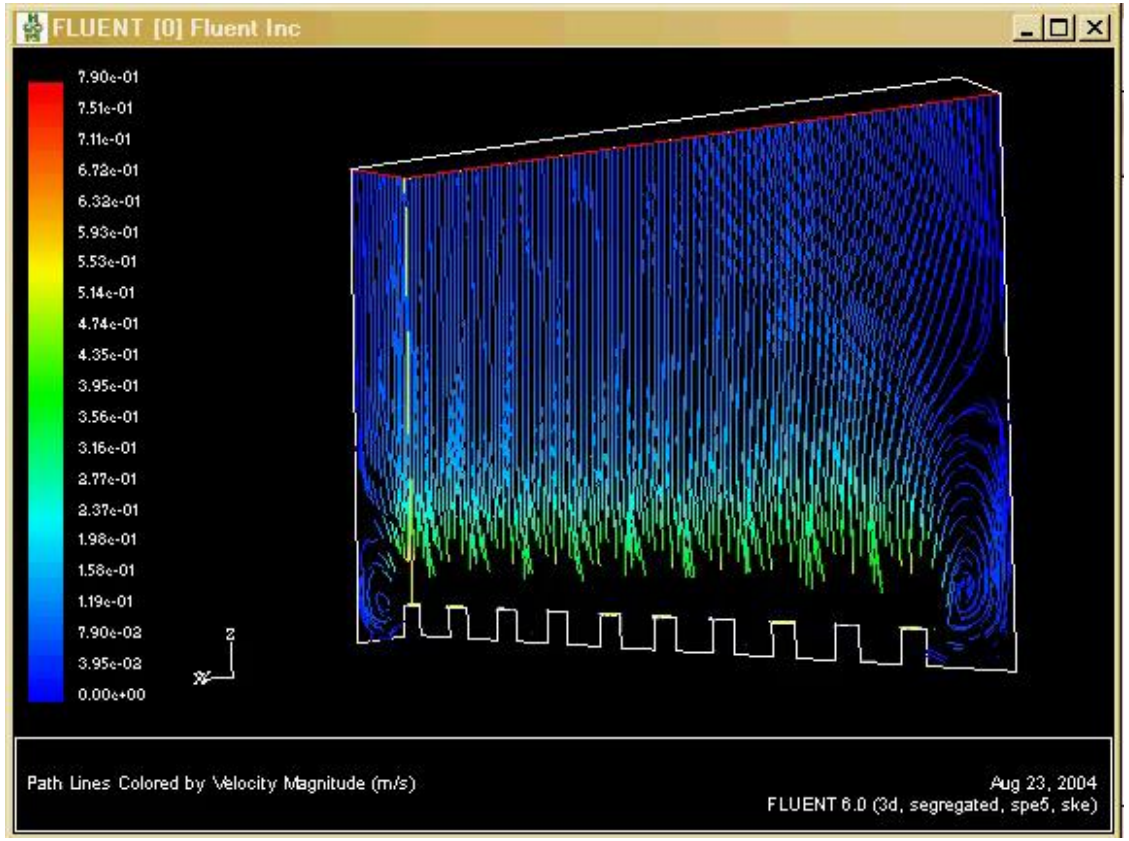

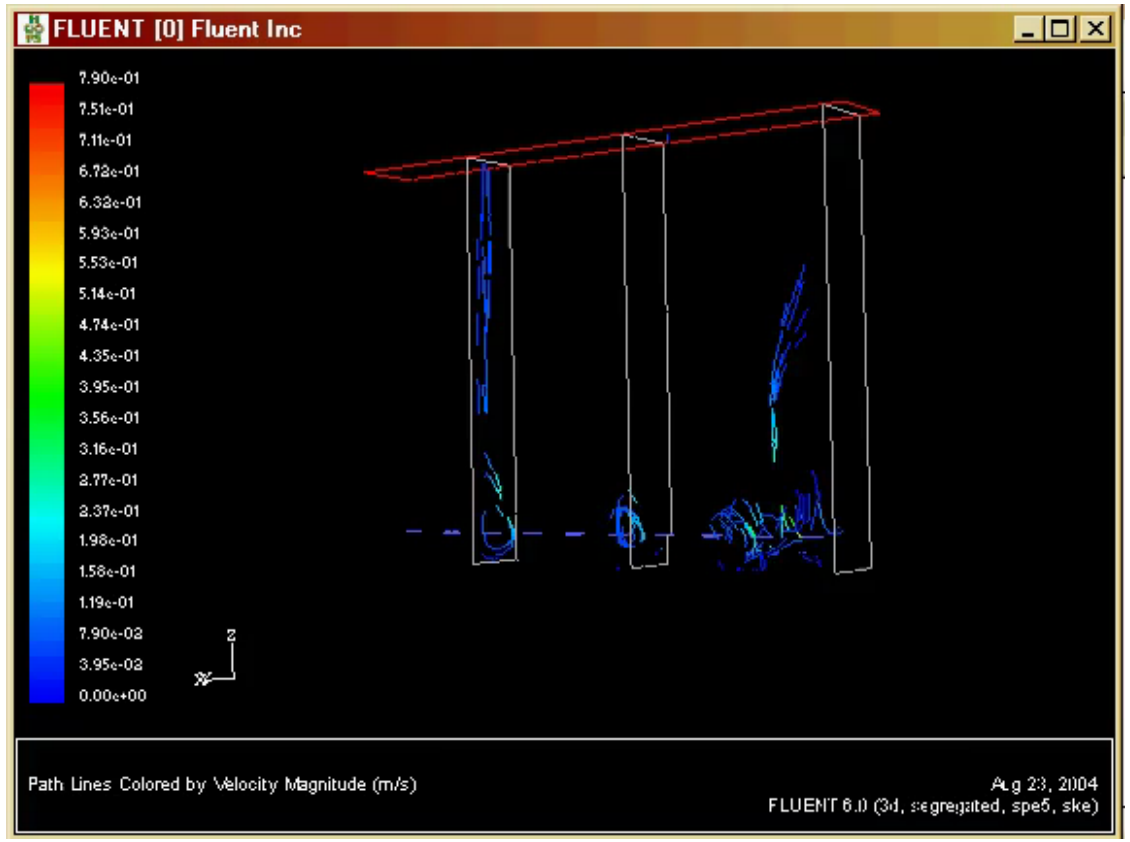

Quemadores tipo flauta

Development of combustion chambers with flute-burners in residential ovens.

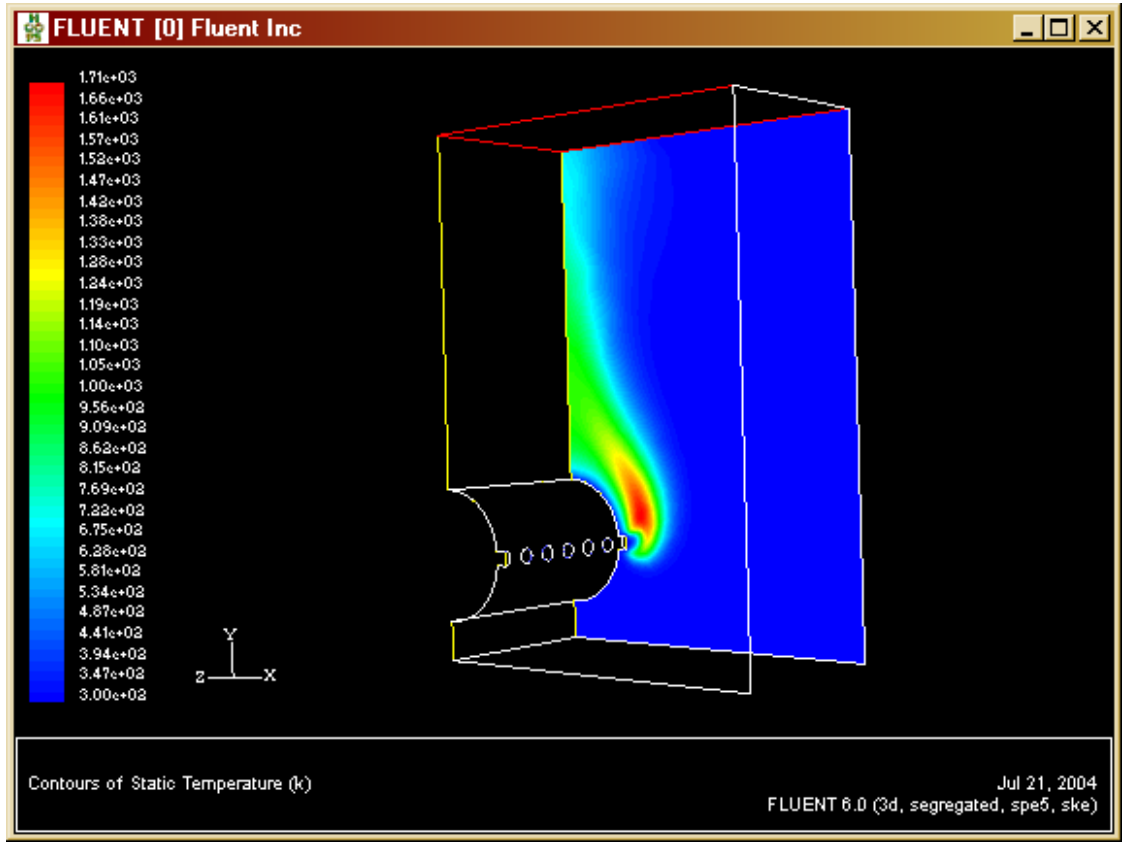

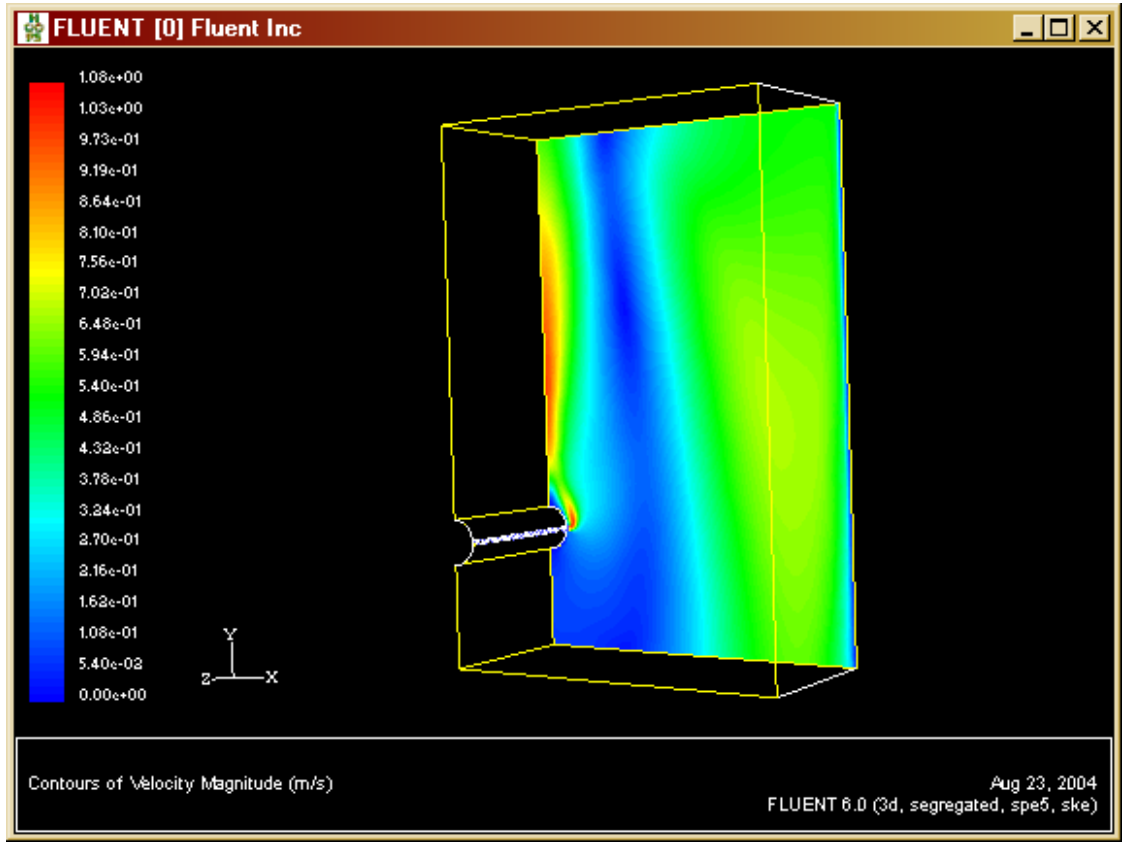

Quemadores tipo flauta

Development of combustion chambers with flute-burners in residential ovens.

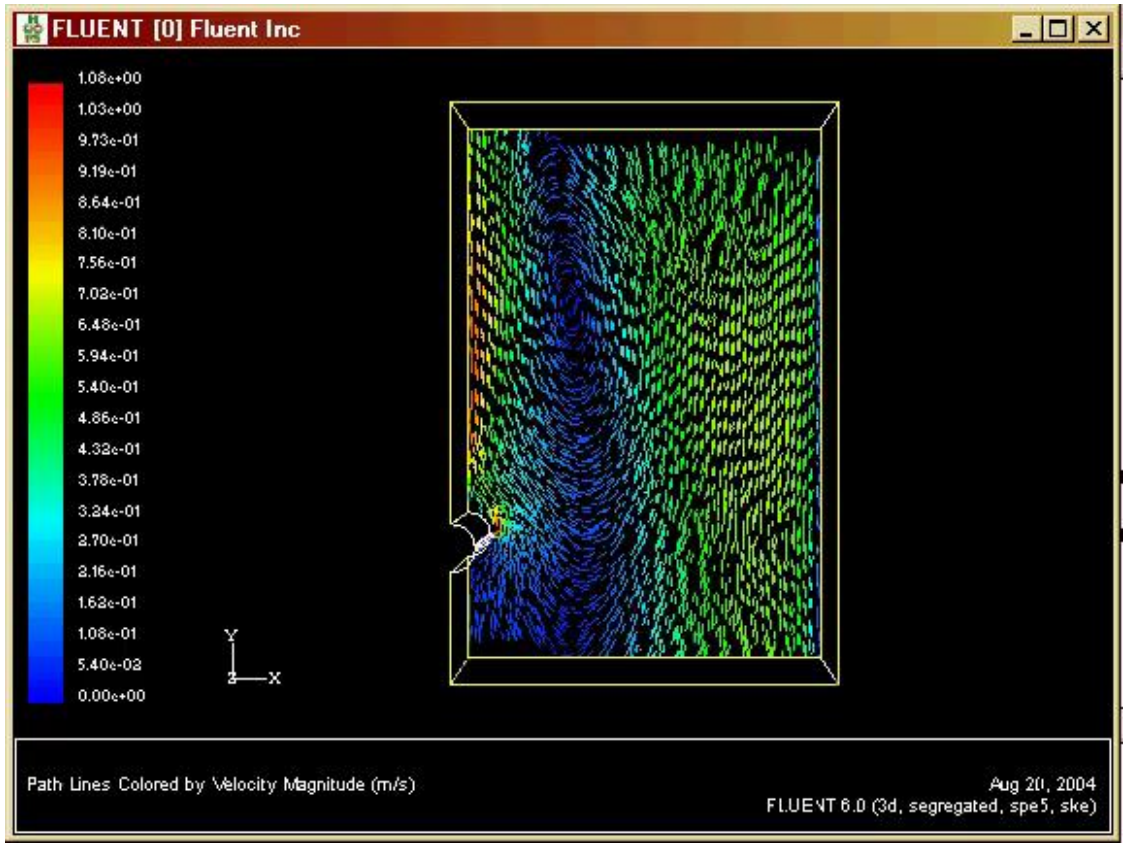

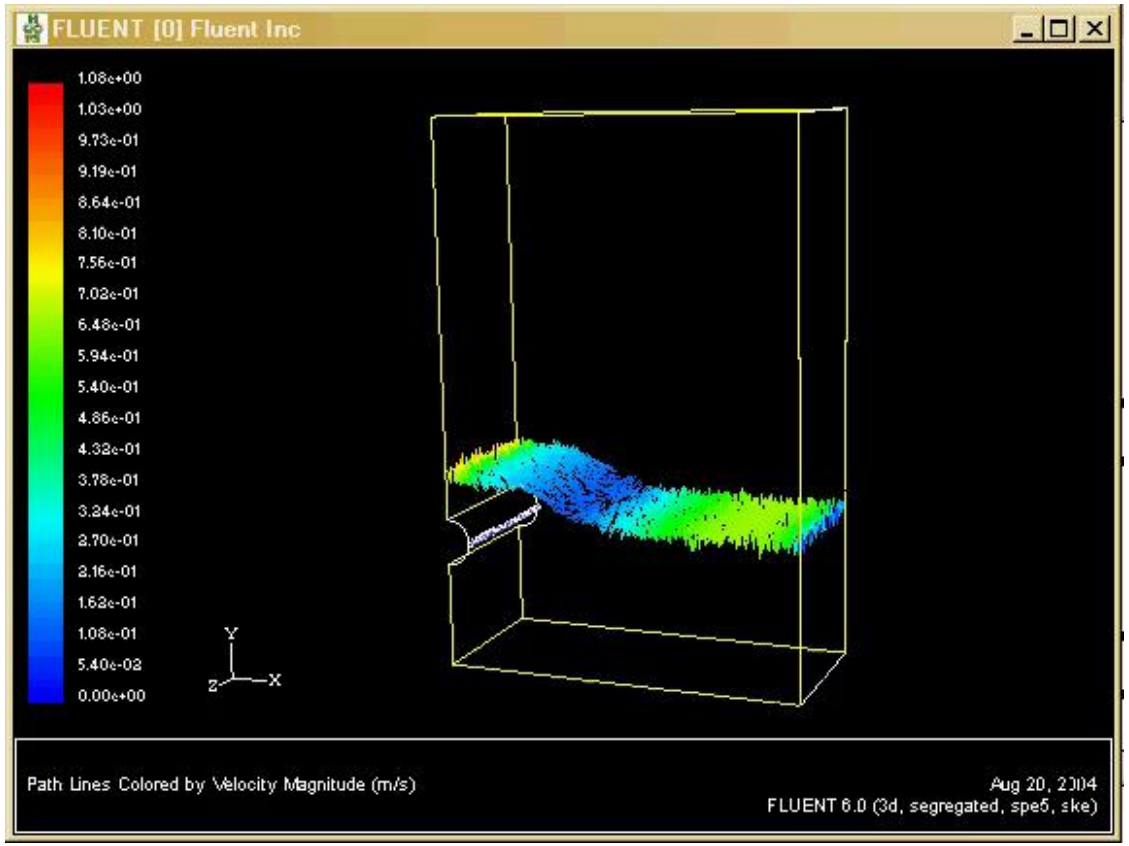

Simulación de un horno residencial

Simulación de un horno residencial

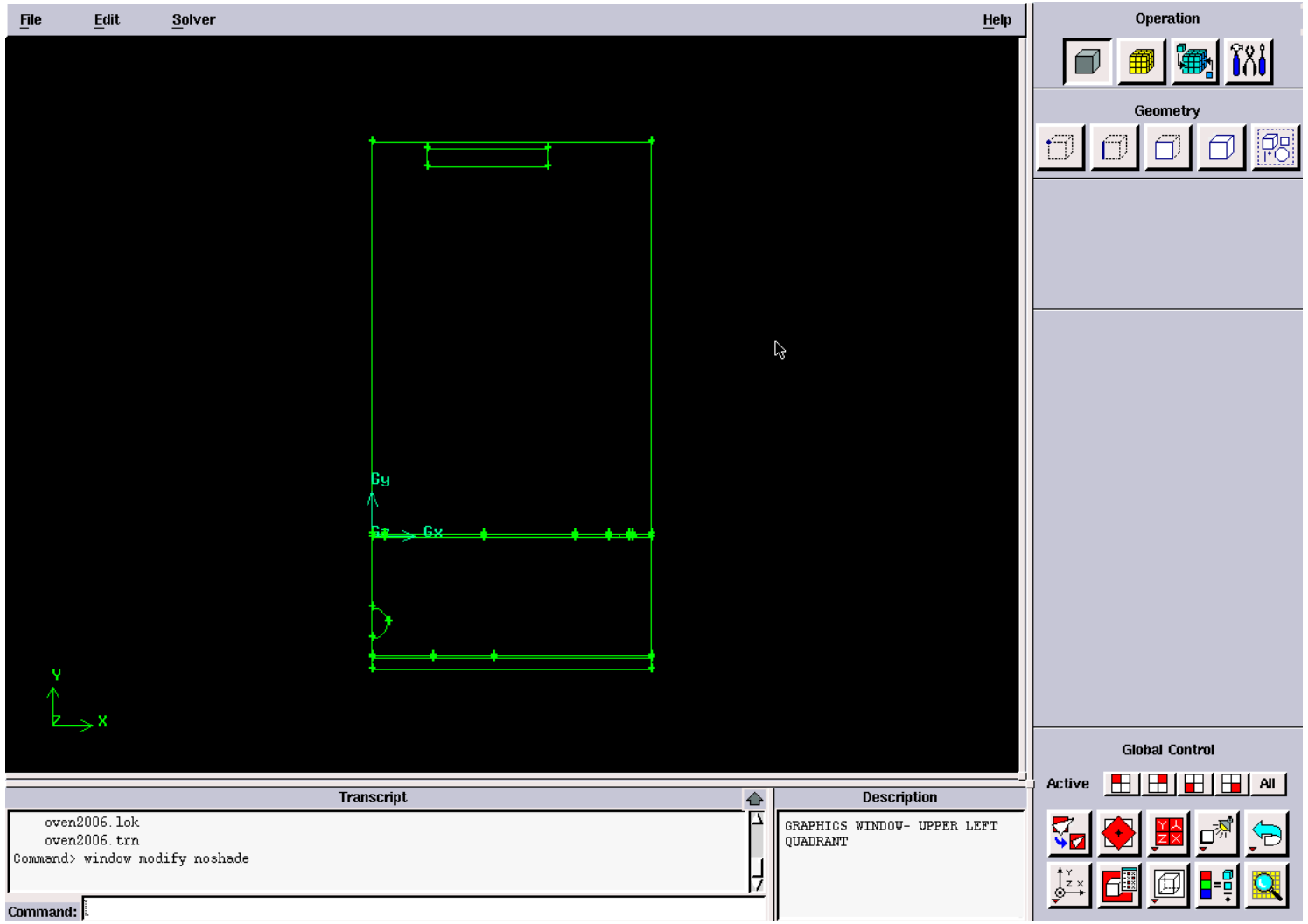

Simulación de un horno residencial

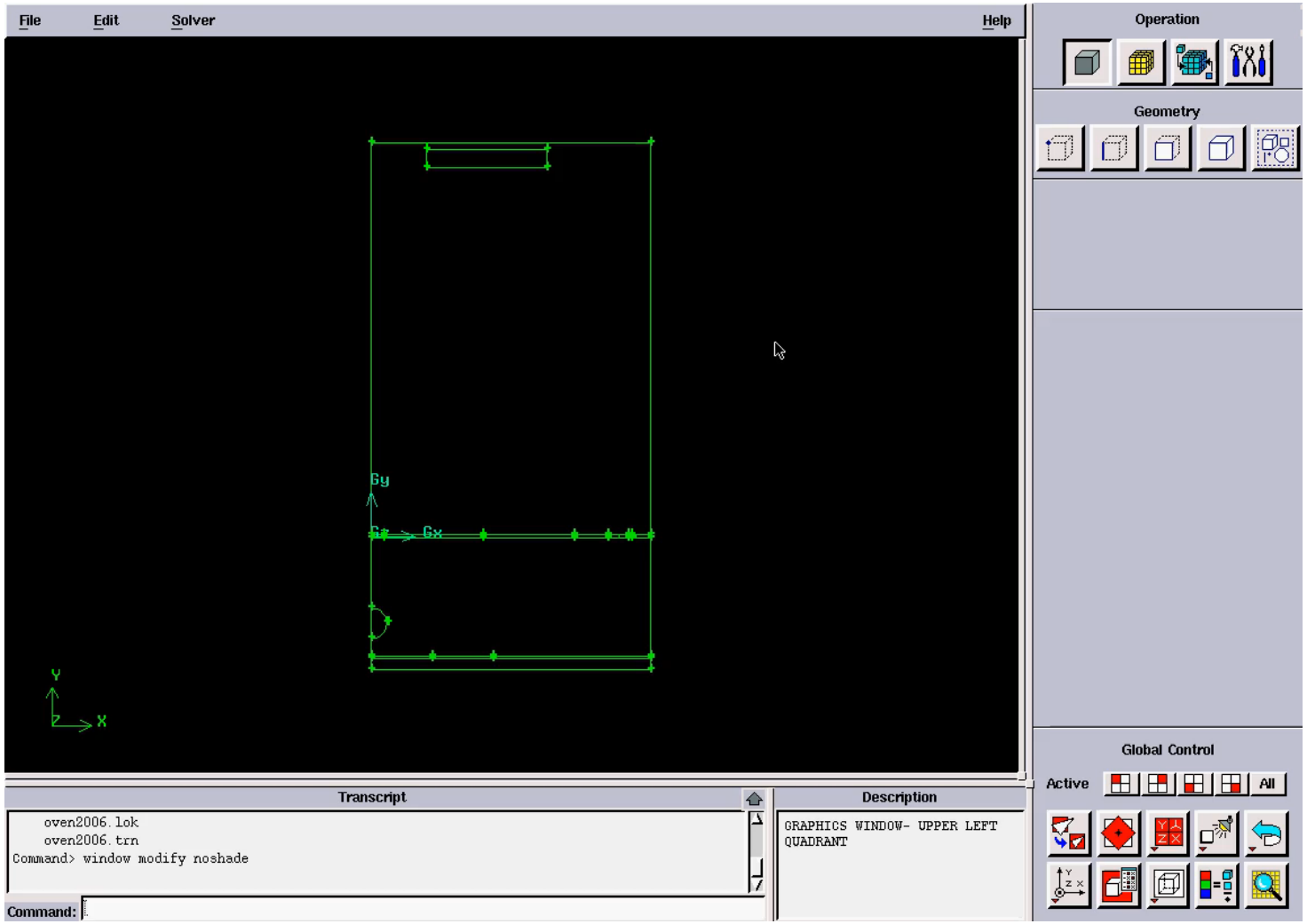

Simulación de un horno residencial

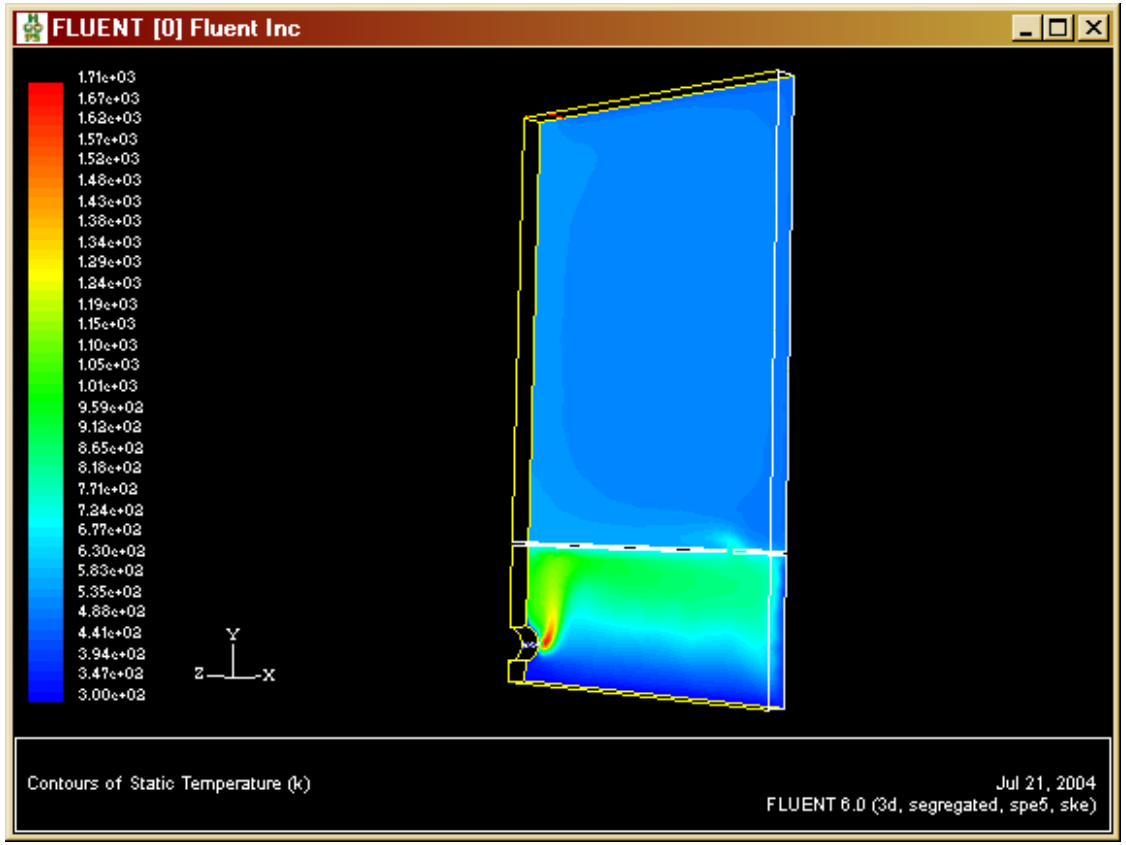

Simulación de un horno residencial

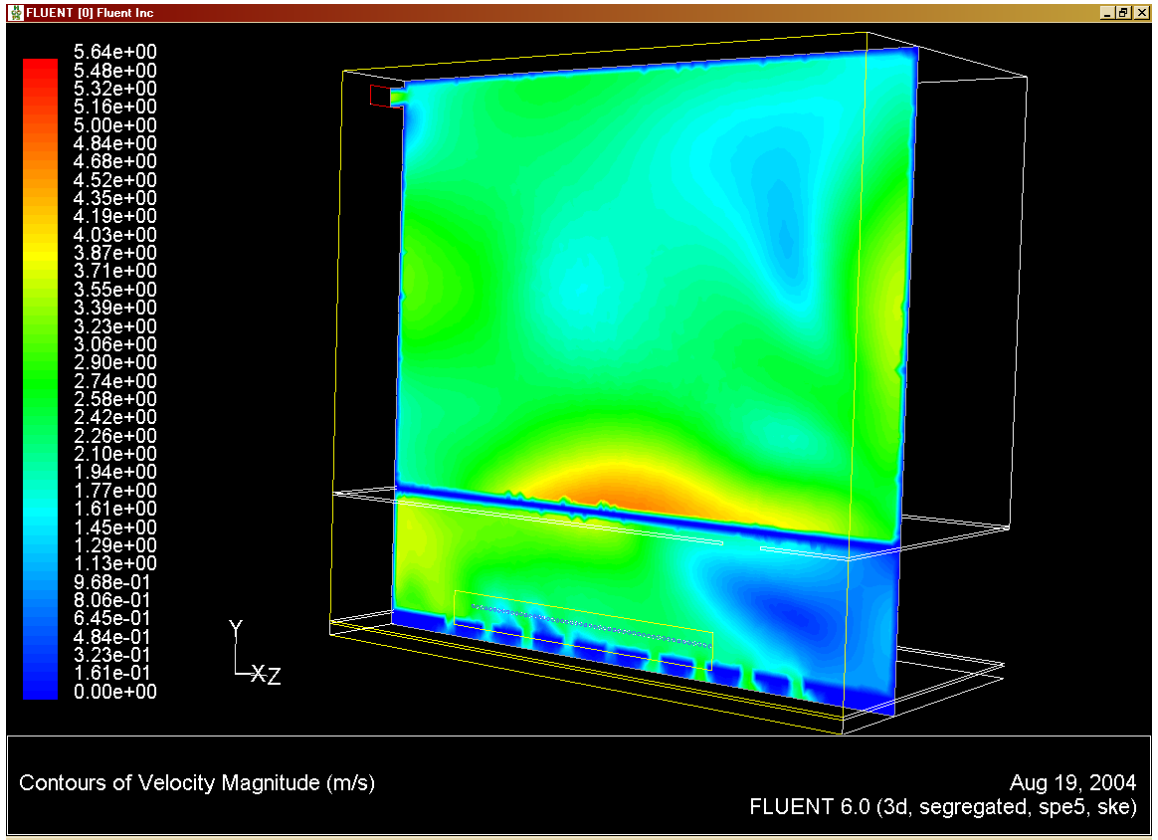

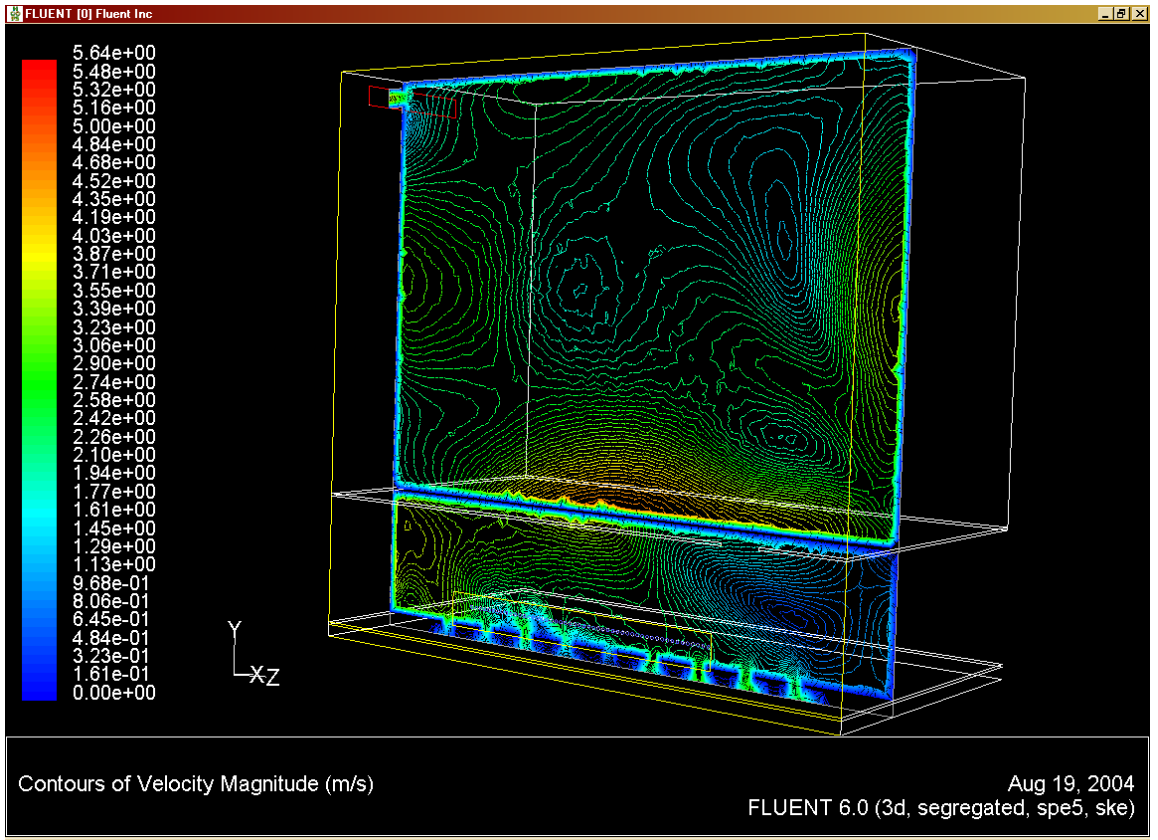

Simulación de un horno residencial

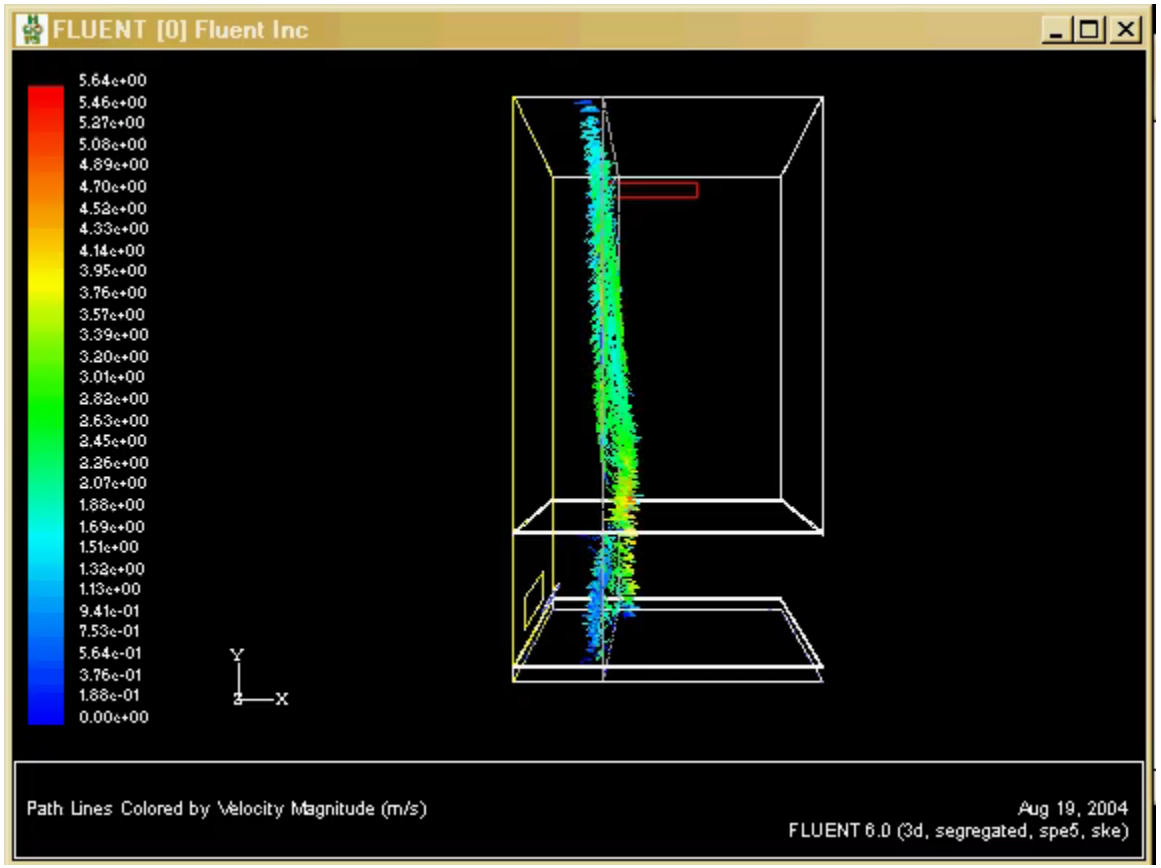

Complejidad numérica y fenológica de la combustión en un MCI

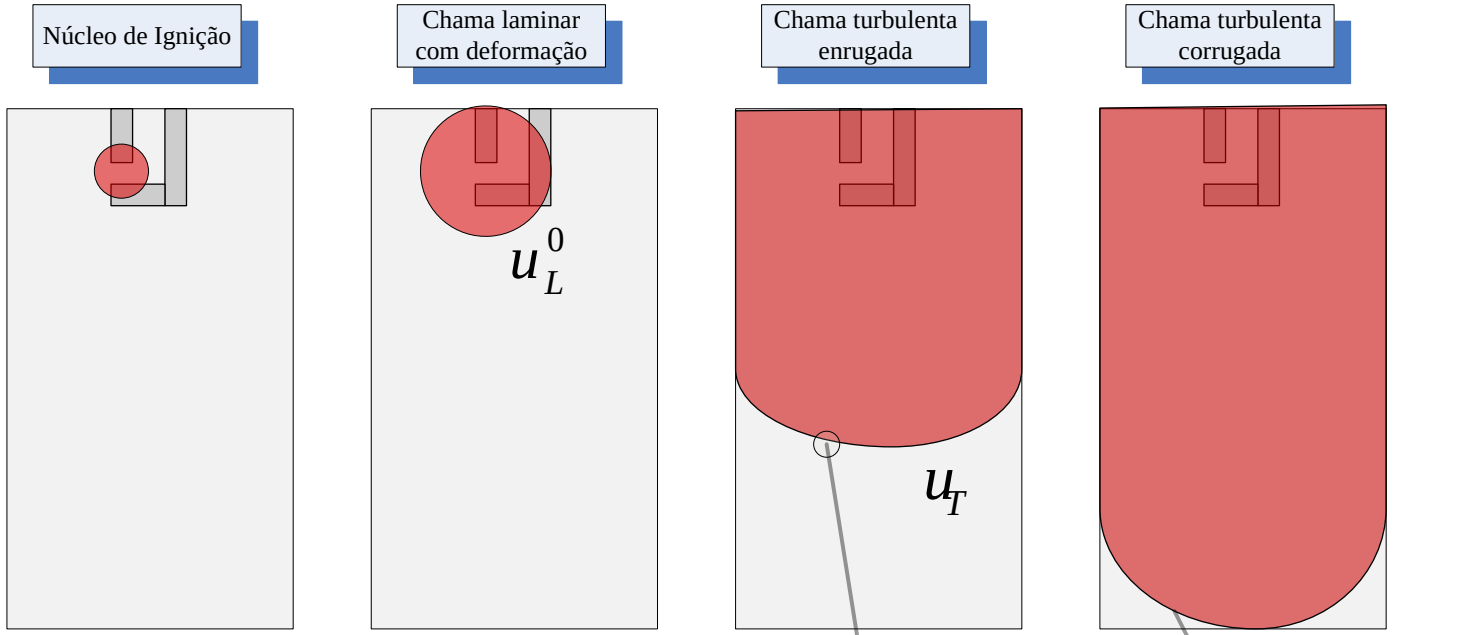

Seqüência de desenvolvimento da combustão em um motor a combustão interna

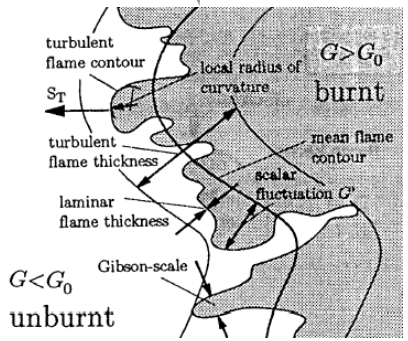

Complejidad numérica y fenológica de la combustión en un MCI

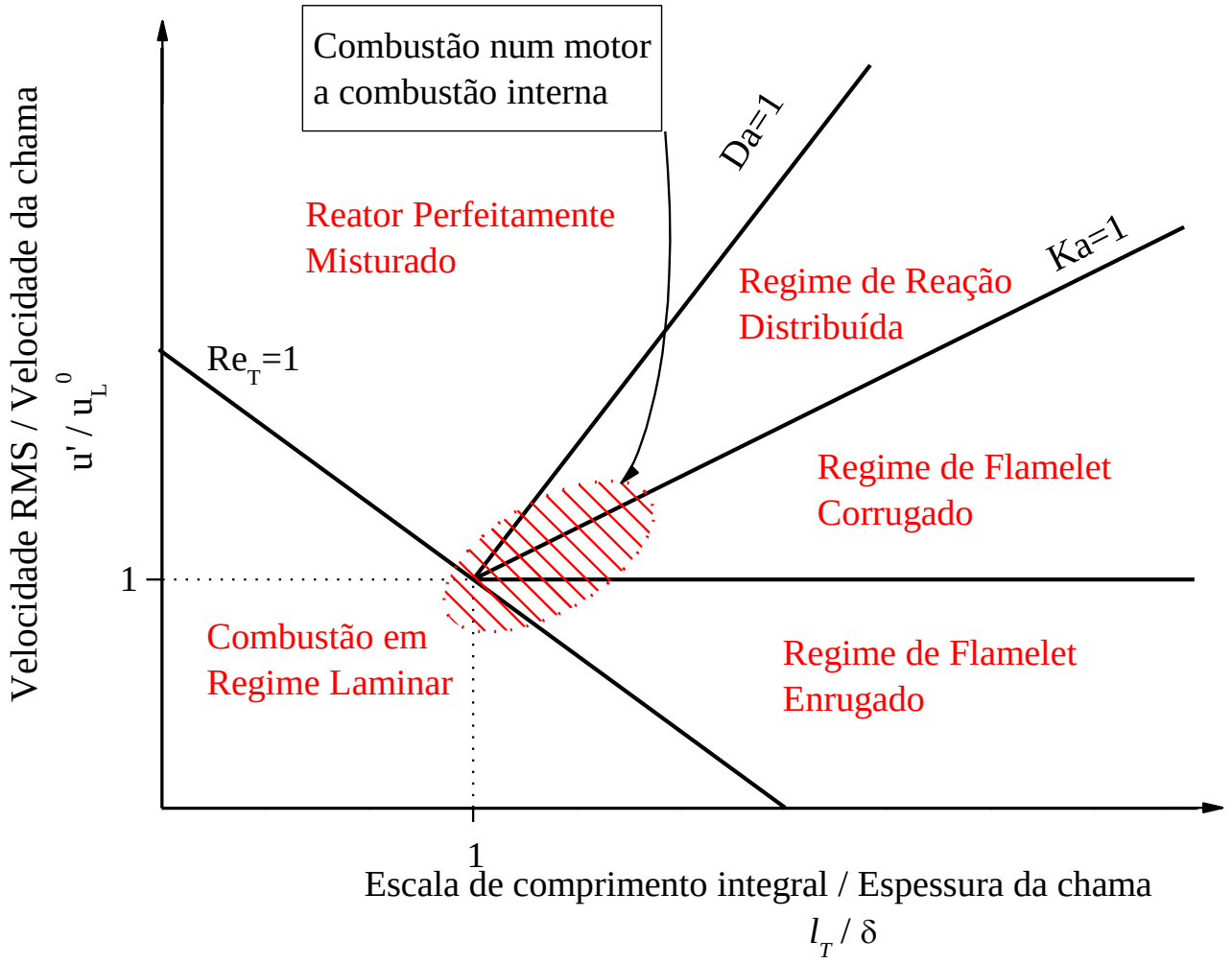

Complejidad numérica y fenológica de la combustión en un MCI

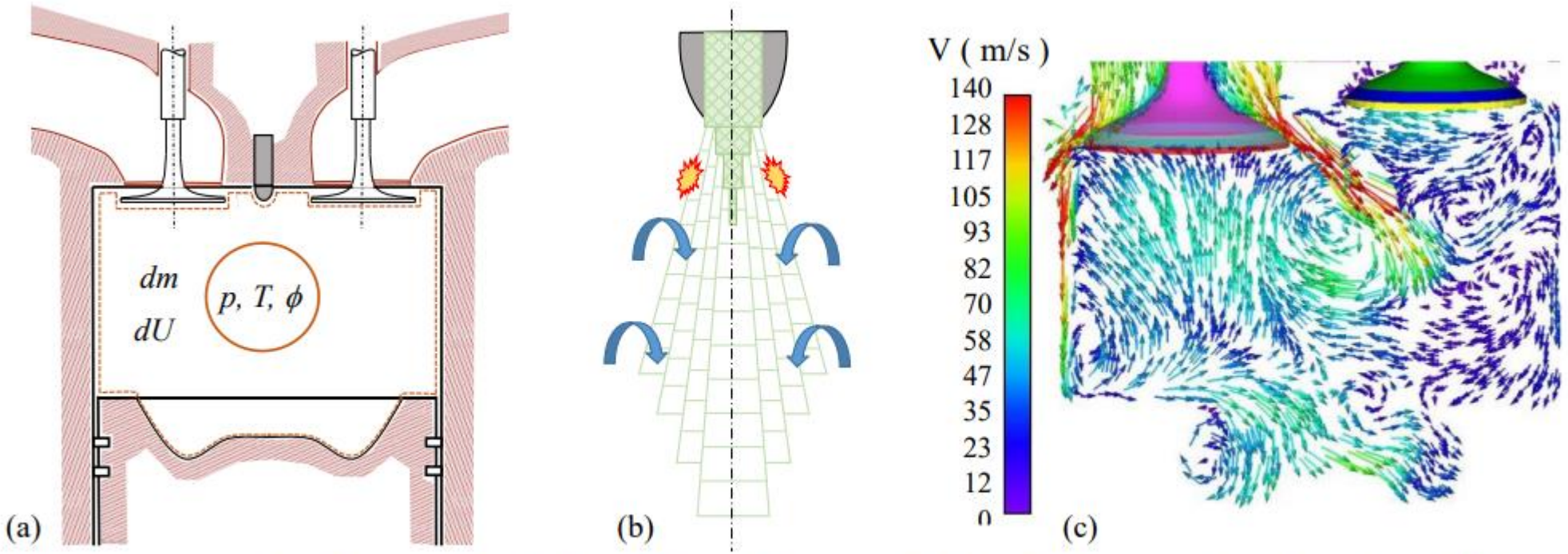

Figure 1. Combustion models - Adapted from Merker *et al.* (2012), figure (c) from Sánchez (2017)

https://repositorio.ufsc.br/bitstream/handle/123456789/229723/COBEM2021_1251.pdf?sequence=1&isAllowed=y

Complejidad numérica y fenológica de la combustión en un MCI

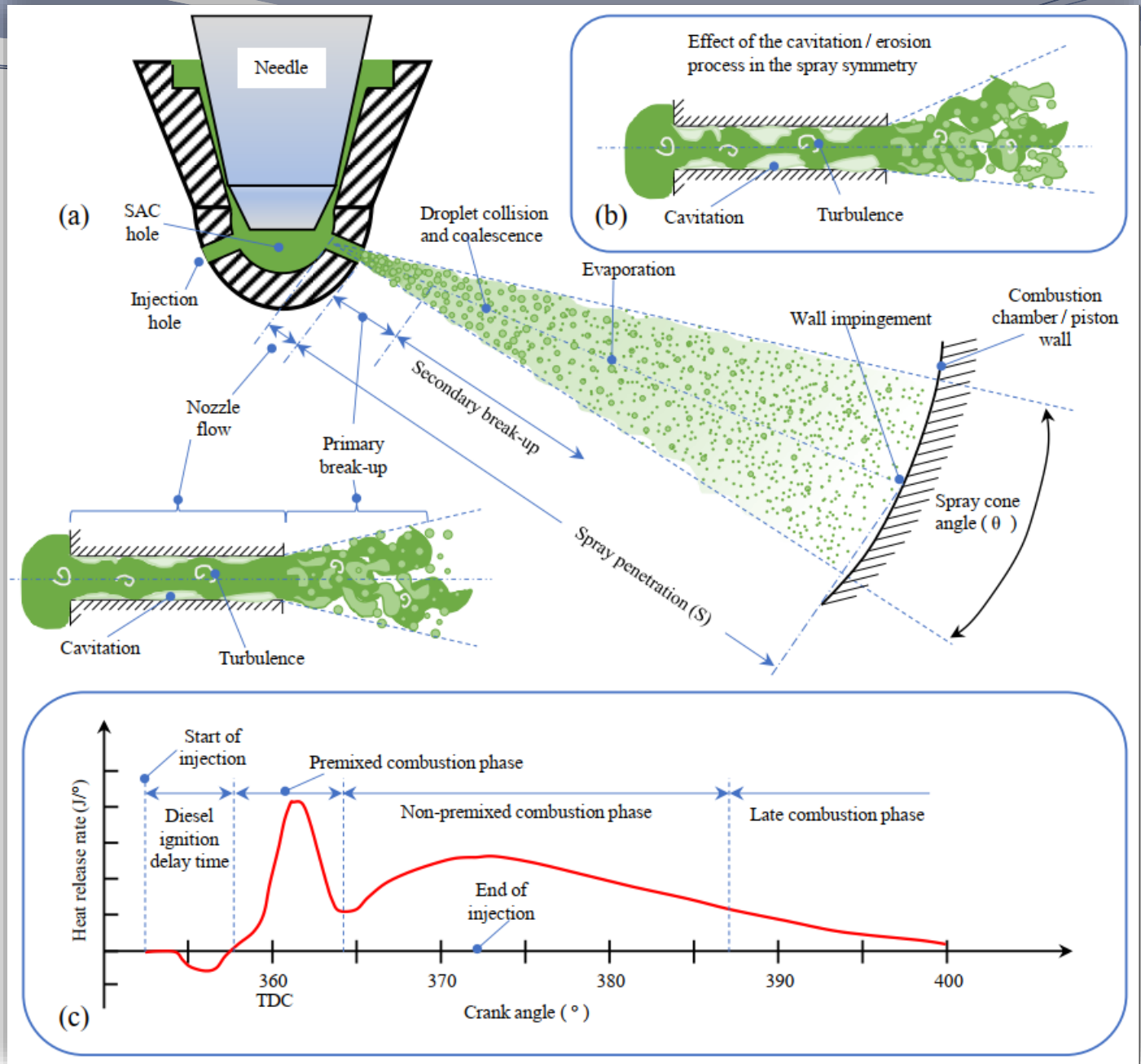

Complejidad numérica y fenológica de la combustión en un MCI

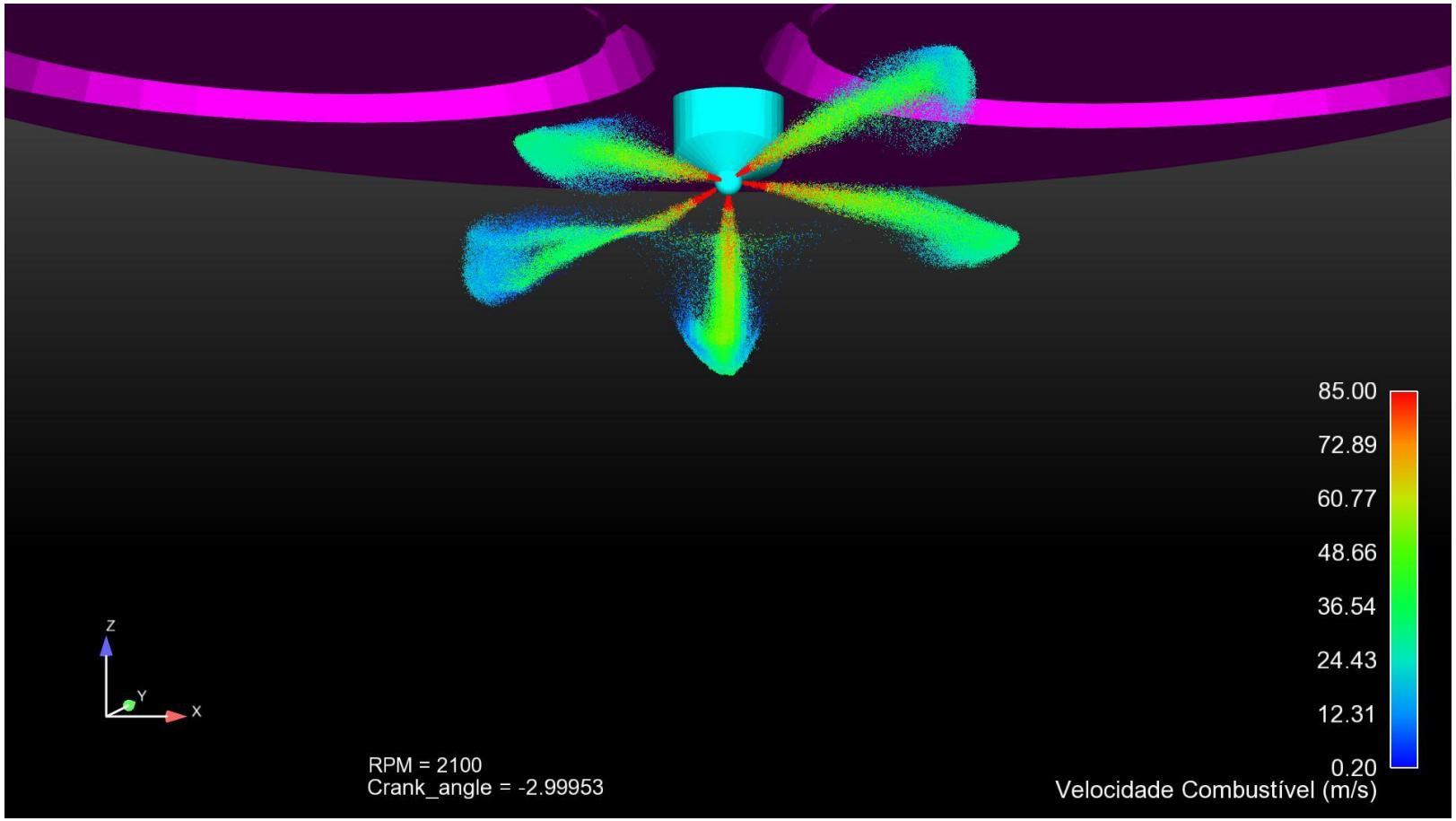

Sánchez, Y.O., 2017. Modelagem e análise numérica da combustão de óleo vegetal in-natura em motores a combustão interna de ignição por compressão. Ph.D. thesis, Federal University of Santa Catarina, Florianópolis, Brasil. URL http://tede.ufsc.br/teses/PEMC1821-T.pdf.

Complejidad numérica y fenológica de la combustión en un MCI

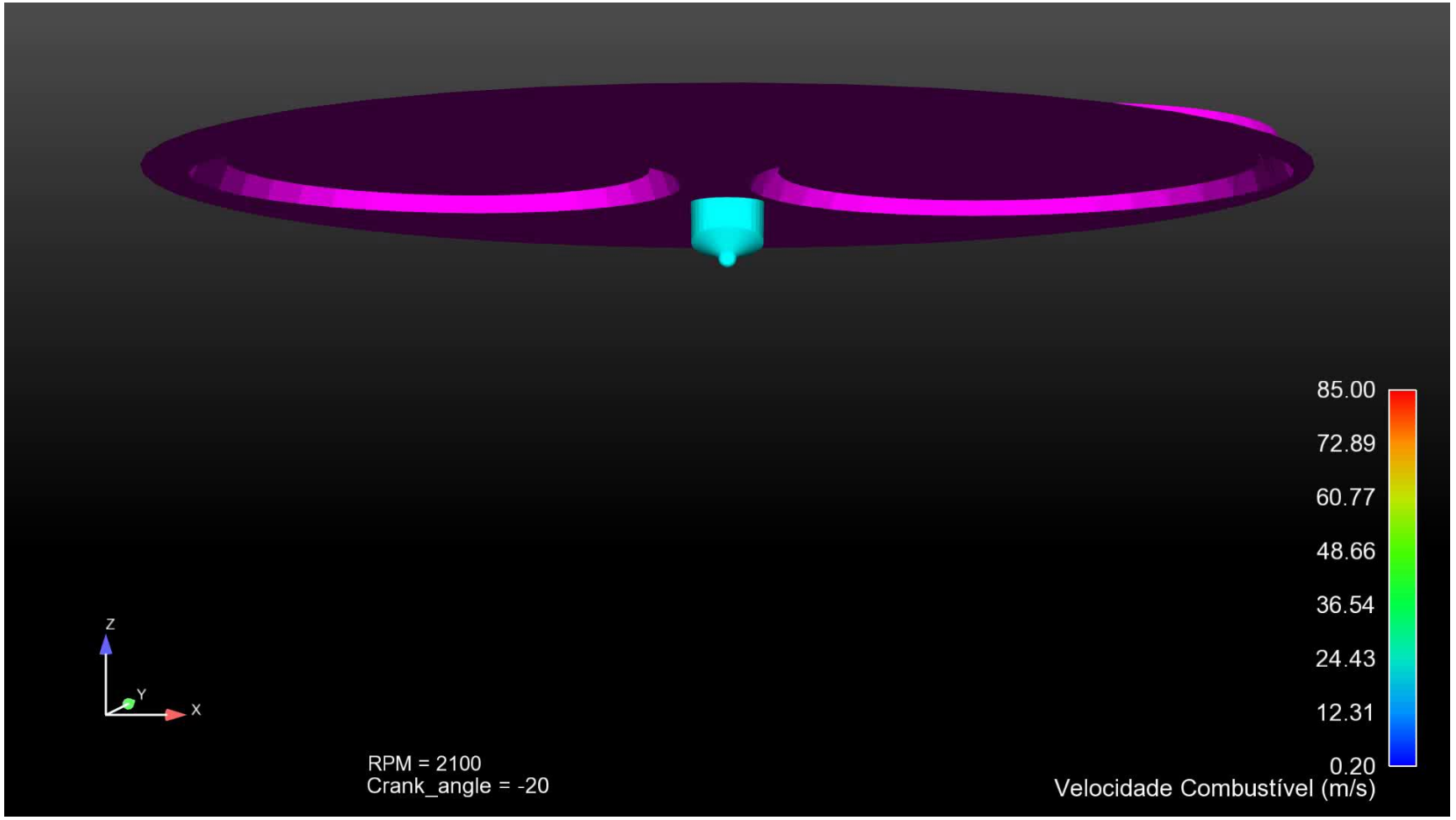

Sánchez, Y.O., 2017. Modelagem e análise numérica da combustão de óleo vegetal in-natura em motores a combustão interna de ignição por compressão. Ph.D. thesis, Federal University of Santa Catarina, Florianópolis, Brasil. URL http://tede.ufsc.br/teses/PEMC1821-T.pdf.

Complejidad numérica y fenológica de la combustión en un MCI

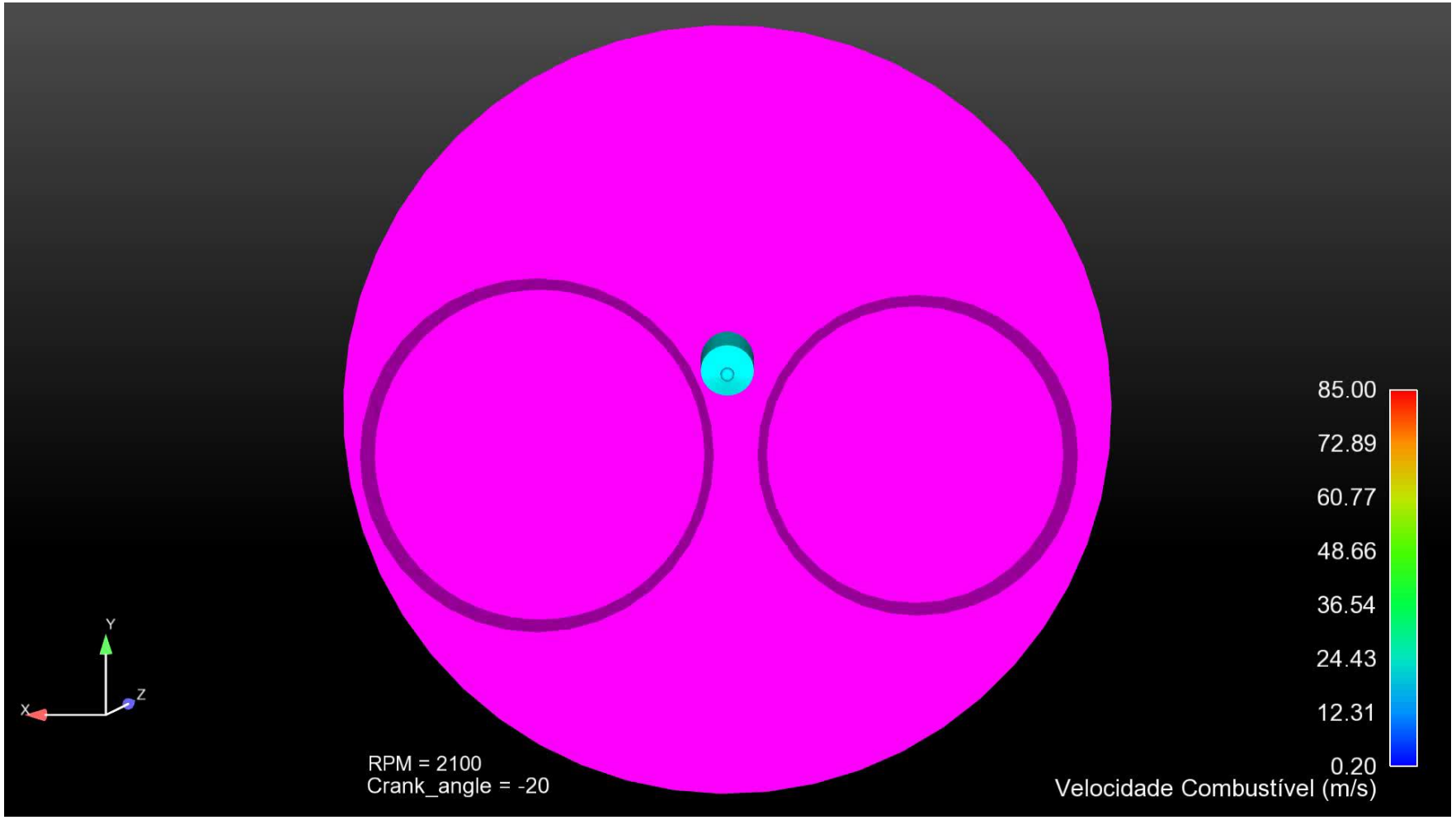

Sánchez, Y.O., 2017. Modelagem e análise numérica da combustão de óleo vegetal in-natura em motores a combustão interna de ignição por compressão. Ph.D. thesis, Federal University of Santa Catarina, Florianópolis, Brasil. URL http://tede.ufsc.br/teses/PEMC1821-T.pdf.

Complejidad numérica y fenológica de la combustión en un MCI

Sánchez, Y.O., 2017. Modelagem e análise numérica da combustão de óleo vegetal in-natura em motores a combustão interna de ignição por compressão. Ph.D. thesis, Federal University of Santa Catarina, Florianópolis, Brasil. URL http://tede.ufsc.br/teses/PEMC1821-T.pdf.

Optimizing fuel spray angle for enhanced efficiency and reducing pollutant emission in diesel locomotive engines

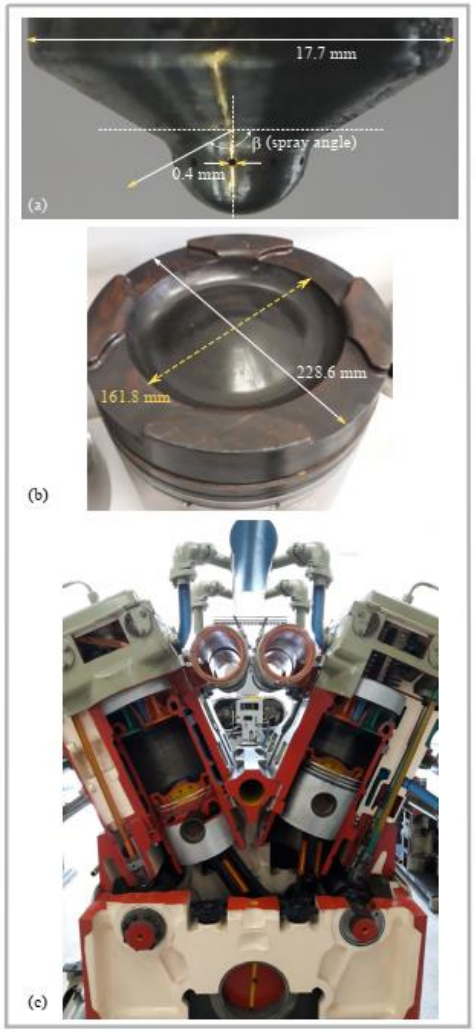

Figure 2: (a) Injector head magnification with main dimensions as input geometrical parameters. (b) Piston head, and (c) Picture of the locomotive GE 7FDL / DASH9-BB40W engine at VALE S.A.

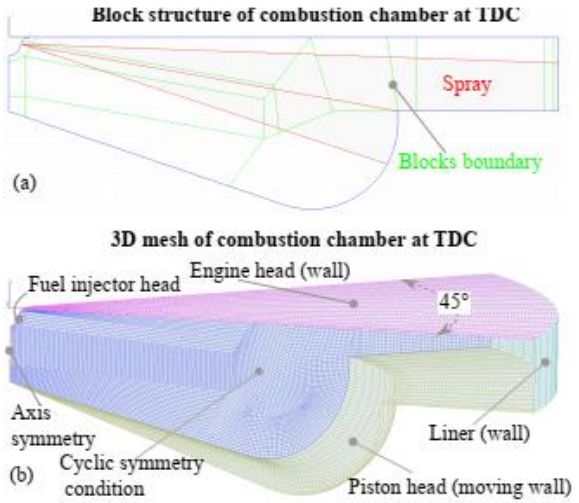

Figure 4: Combustion chamber geometry modeled at top dead center. (a) Block-structured mesh; (b) 3D combustion chamber model at TDC and boundary conditions. ($\beta = 160°$)

Table 3: Initial conditions used for simulations of the DASH9-BB40W engine reproduced in this work, for all the spray angles (β) investigated in this work

Parameter	Description
Engine speed	996 rpm ‡
Cylinder pressure	255000 Pa ‡
Movement wall temp.	570.15 K *
Fixed wall temperature	470.15 K ‡
Air temp.	355 K ‡
Fuel	Diesel-D1
Fuel temperature	350 K ‡
Injected mass	1.10E-03 kg ‡
Start of injection (SOI)	342° ‡
Injection duration	6.35 ms ‡
Injection timing	698 - 706 ($\Delta = 2$) CA ‡
EGR Mass fraction	0.049 †
Swirl	2880 1/min †
Turbulent length scale	0.0045 m †
Turbulent kinetic energy	10 m^2/s^2 †

‡ experimental data from [27]
* parameter used for model calibration.
† recommended values from [28]

Table 4: Sub-models used in the AVL-FIRE™ ESE DIESEL simulations

Models	
Combustion	
Coherent Flame Model / ECFM-3Z	[37] [38]
Turbulence	
κ-ζ-f	[39] [40] [41]
Emission	
Extended Zeldovich NO model	[30] [31] [42]
Soot model (Kinetic Model)‡	[28]
Spray	
Drag law model (Schiller Naumann)	[43]
Wall interaction model (Wall Jet 1)	[44]
Evaporation model (Dukowicz)	[45]
Breakup model (Wave)	[33]

‡ Soot model available in the AVL-FIRE™ ESE DIESEL simulation package

Optimizing fuel spray angle for enhanced efficiency and reducing pollutant emission in diesel locomotive engines

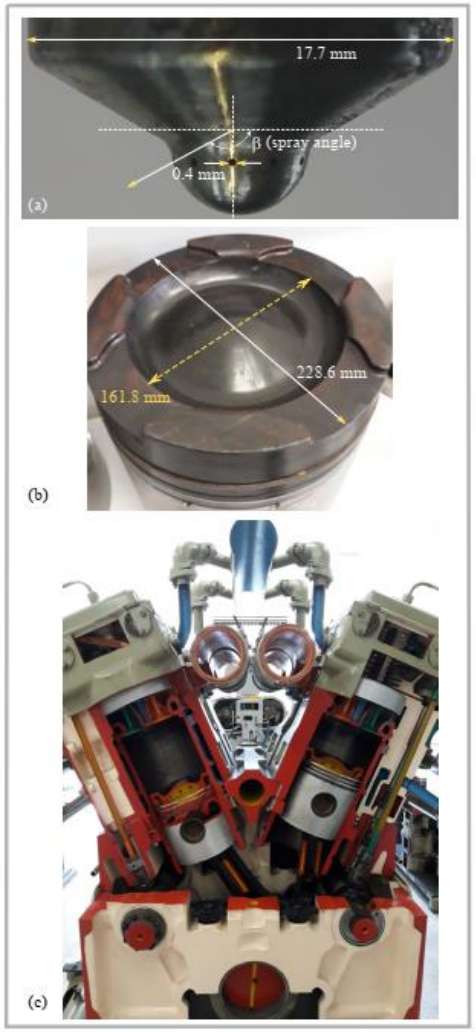

Figure 2: (a) Injector head magnification with main dimensions as input geometrical parameters. (b) Piston head, and (c) Picture of the locomotive GE 7FDL / DASH9-BB40W engine at VALE S.A.

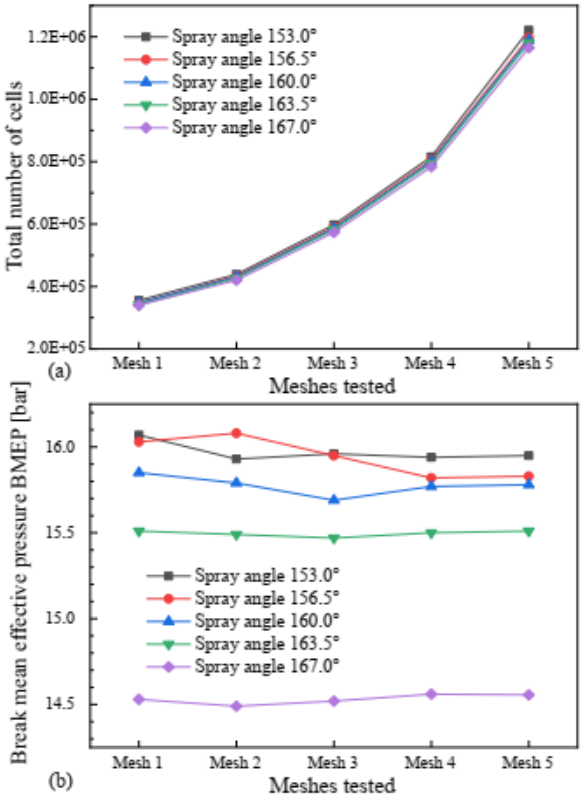

Figure 5: Mesh independence test results for the spray angles investigated in this work, at default engine injection timing (702 CA). (a) Total number of cells for each spray angle (β), for each mesh tested. (b) Behavior in terms of break mean effective pressure prediction of all the meshes tested.

Table 5: Averaged measured parameters, per piston - DASH 9 BB40W - locomotive "A". [27]

	Mean break effective pressure BMEP [bar]	Indicated power [kW]
Average†	15.79	154.17
Maximum*	16.96	169.27
Minimum*	14.13	140.88

† Data obtained along the whole measurement time

* Data observed locally on time as maximum or minimum

Table 6: Numerical predictions in terms of mean break effective pressure and indicated power for all the spray angles (β) and injection timing investigated in this work

Spray angle β	Mean break effective pressure BMEP [bar]	Indicated power [kW]
Injection timing = 698 CA		
153.0°	16.23	148.44
156.5°	16.23	148.41
160.0° †	16.02	146.58
163.5°	15.44	141.24
167.5°	14.49	132.69
Injection timing = 700 CA		
153.0°	15.94	145.78
156.5°	15.83	144.78
160.0° †	15.77	144.26
163.5°	15.61	142.80
167.5°	14.57	133.36
Injection timing = 702 CA		
153.0°	15.98	145.78
156.5°	15.93	144.74
160.0° †	15.85	144.25
163.5°	15.61	141.81
167.5°	14.67	133.24
Injection timing = 704 CA		
153.0°	15.94	145.78
156.5°	15.83	144.78
160.0° †	15.62	142.92
163.5°	15.41	140.97
167.5°	14.59	133.53
Injection timing = 706 CA		
153.0°	15.94	145.78
156.5°	15.83	144.78
160.0° †	15.77	144.26
163.5°	15.20	139.11
167.5°	14.52	132.94

† Fuel spray angle of the DASH 9 BB40W locomotive "A". [12]

Optimizing fuel spray angle for enhanced efficiency and reducing pollutant emission in diesel locomotive engines

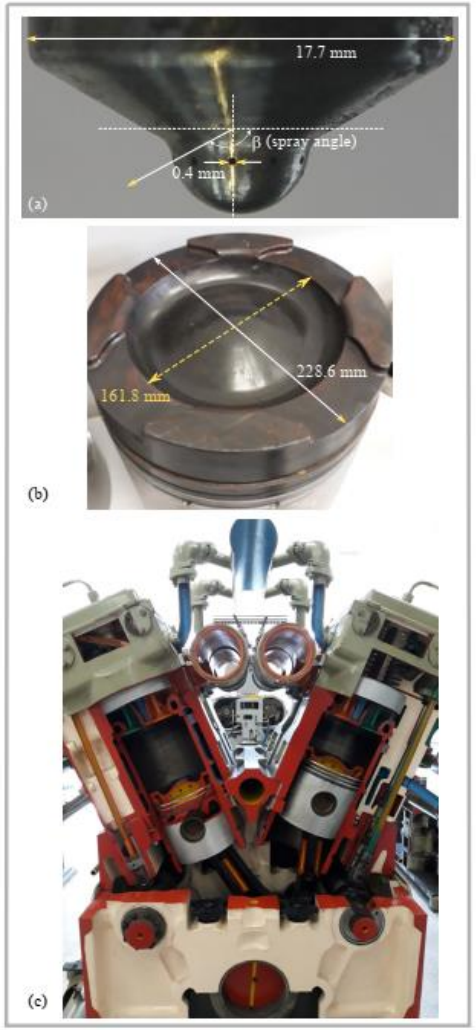

Figure 2: (a) Injector head magnification with main dimensions as input geometrical parameters. (b) Piston head, and (c) Picture of the locomotive GE 7FDL / DASH9-BB40W engine at VALE S.A.

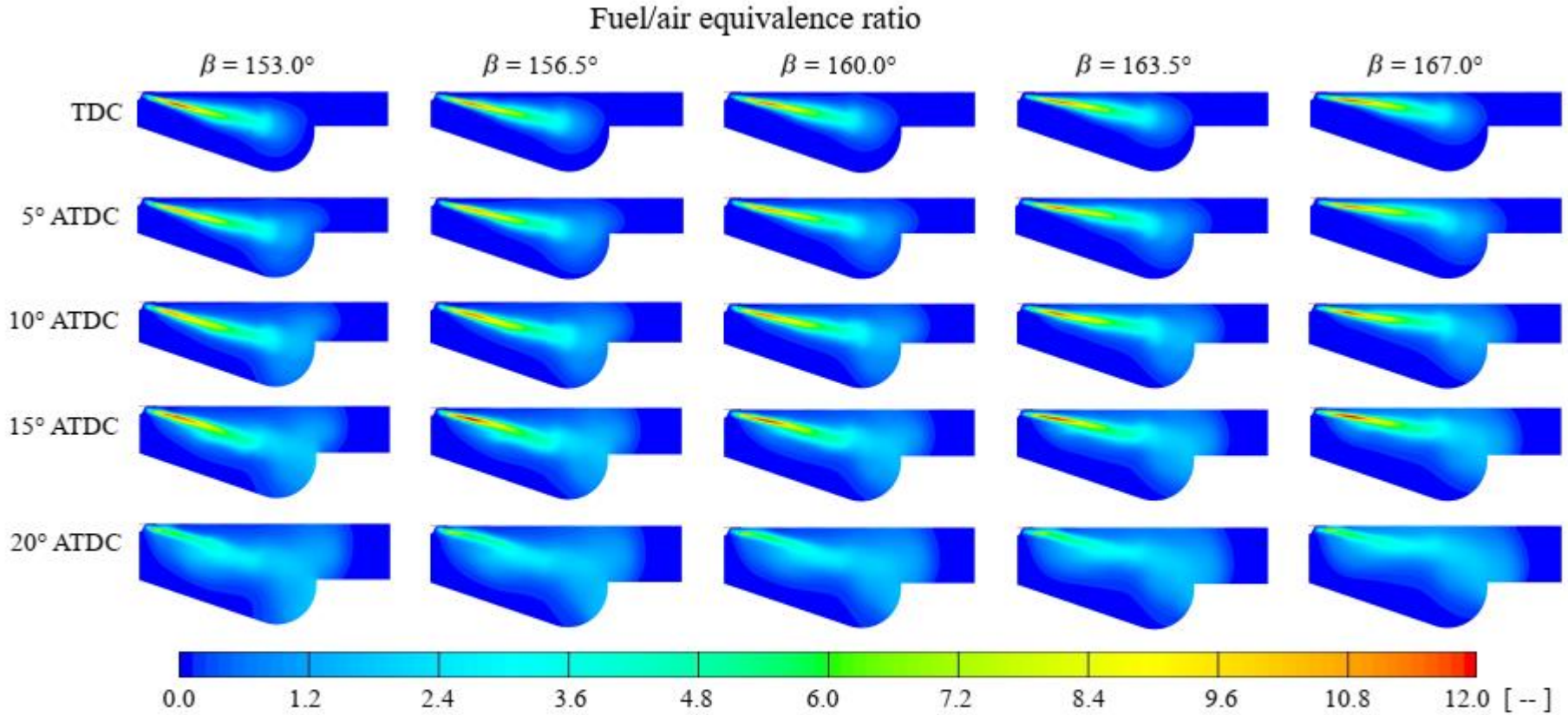

Figure 7: Fuel / Air equivalence ratio fields for all the spray angles (β) investigated in this work, along the first 20° crank angle after top dead center ($\Delta CA = 5°$), at default engine injection timing (702 CA).

Optimizing fuel spray angle for enhanced efficiency and reducing pollutant emission in diesel locomotive engines

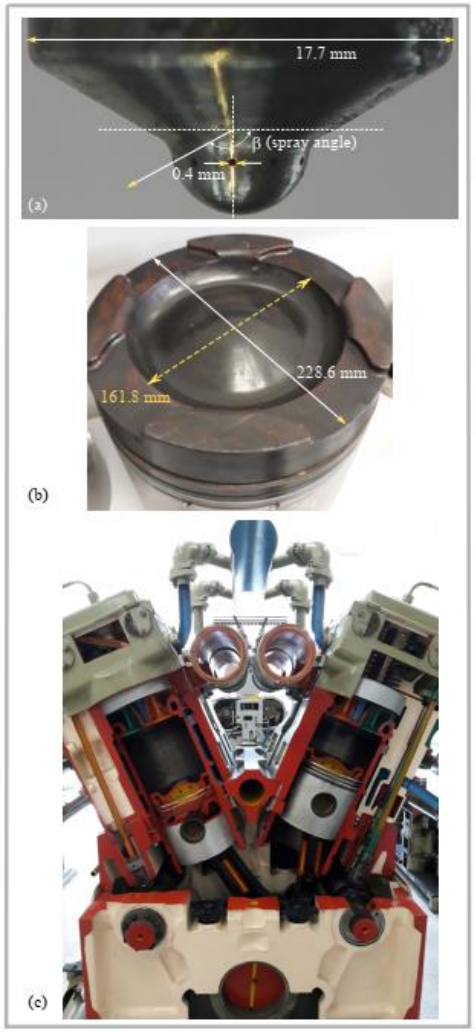

Figure 2: (a) Injector head magnification with main dimensions as input geometrical parameters. (b) Piston head, and (c) Picture of the locomotive GE 7FDL / DASH9-BB40W engine at VALE S.A.

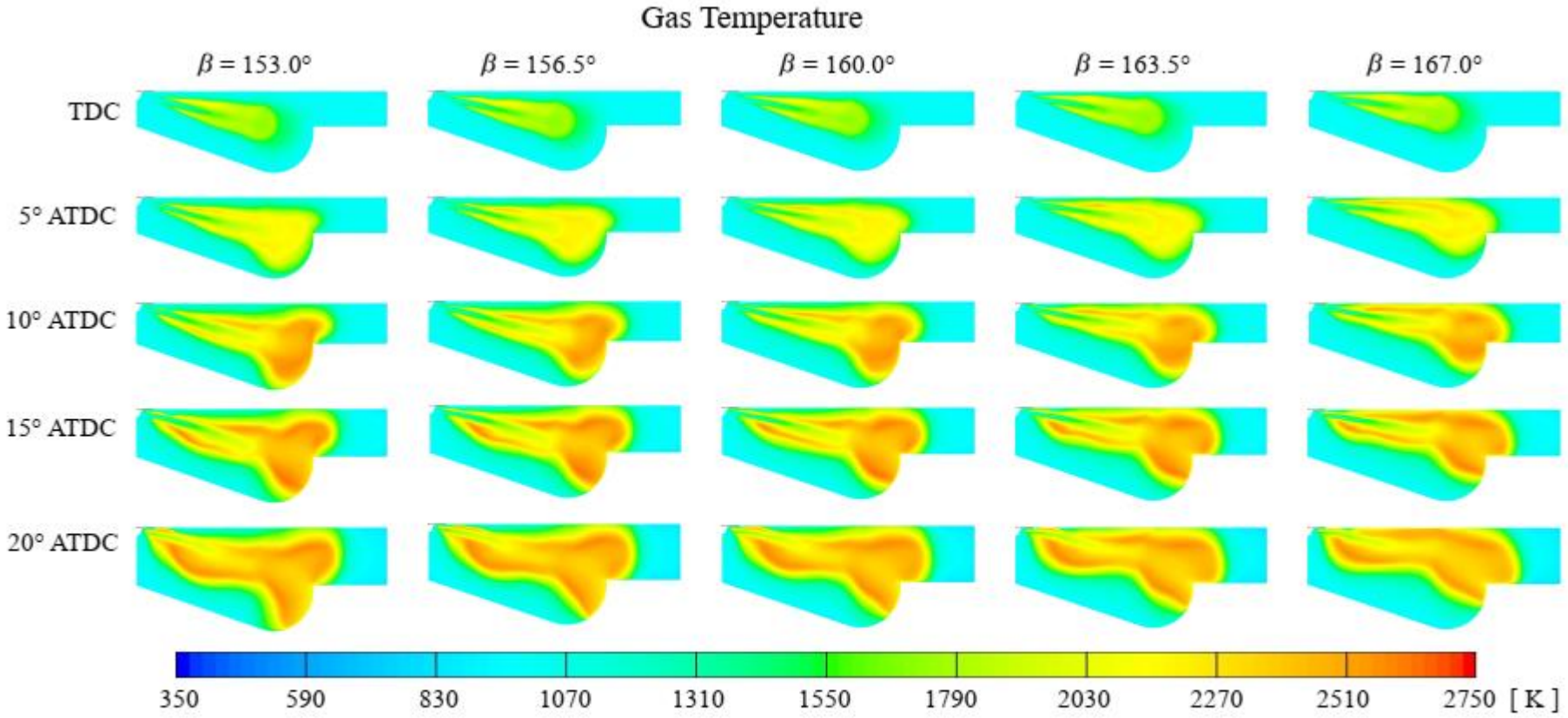

Figure 8: Gas temperature fields for all the spray angles (β) investigated in this work, along the first 20° crank angle after top dead center ($\Delta CA = 5°$), at default engine injection timing (702 CA).

Optimizing fuel spray angle for enhanced efficiency and reducing pollutant emission in diesel locomotive engines

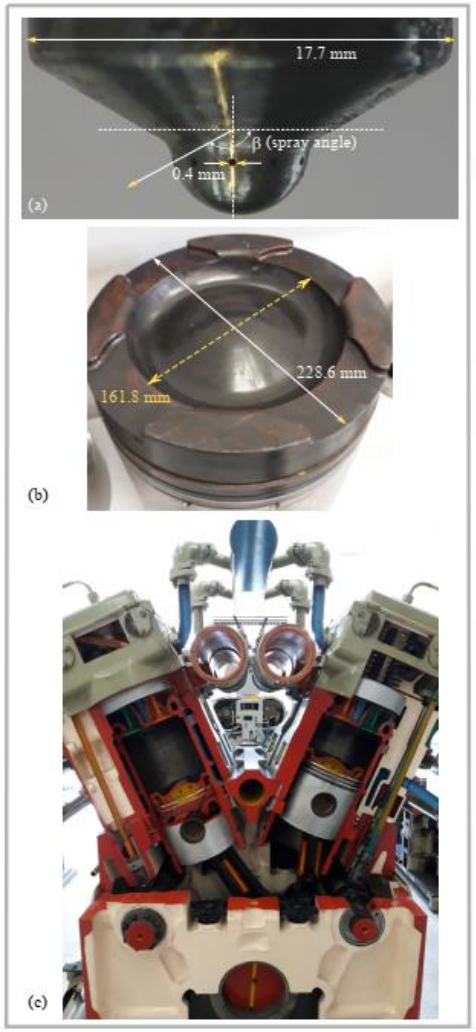

Figure 2: (a) Injector head magnification with main dimensions as input geometrical parameters. (b) Piston head, and (c) Picture of the locomotive GE 7FDL / DASH9-BB40W engine at VALE S.A.

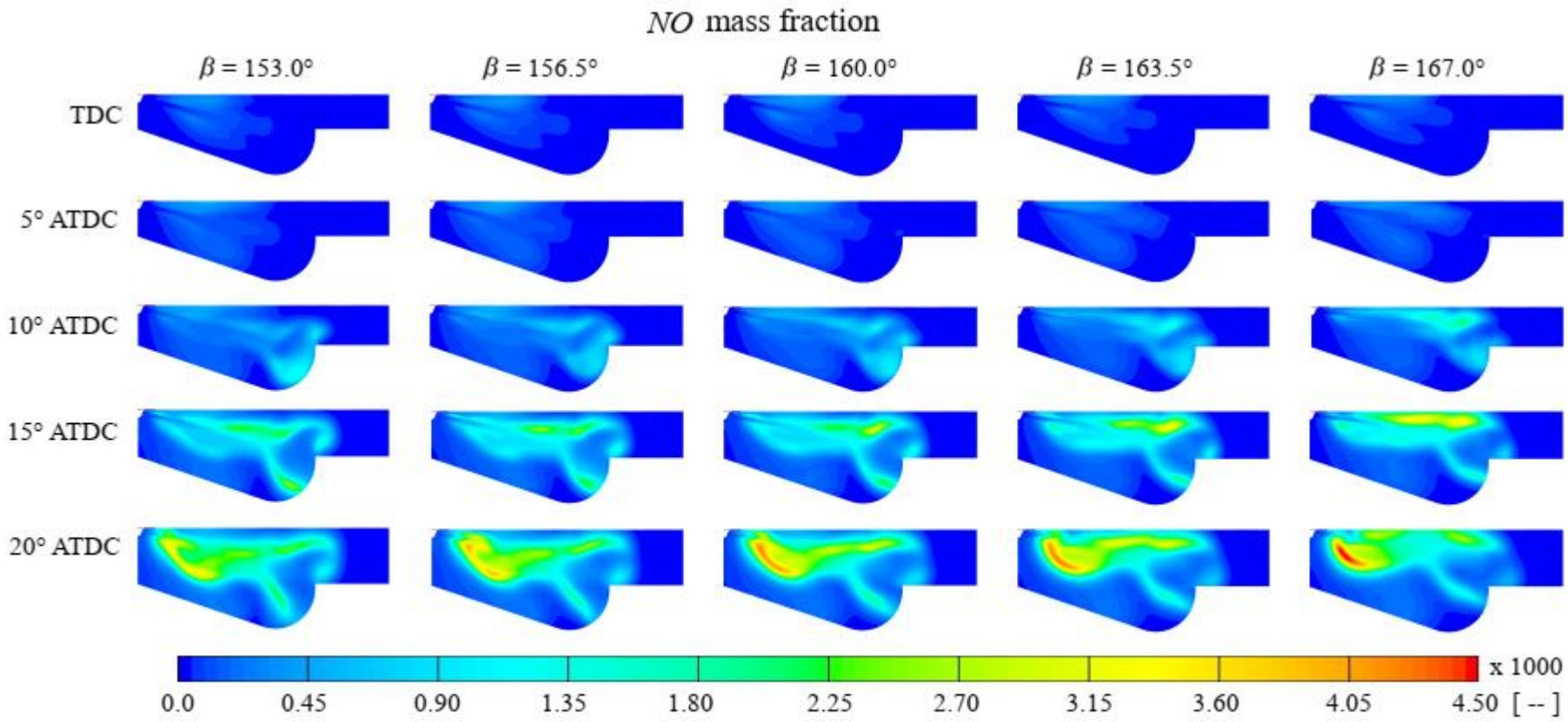

Figure 9: *NO* mass fraction fields for all the spray angles (β) investigated in this work, along the first 20° crank angle after top dead center ($\Delta CA = 5°$), at default engine injection timing (702 CA).

Optimizing fuel spray angle for enhanced efficiency and reducing pollutant emission in diesel locomotive engines

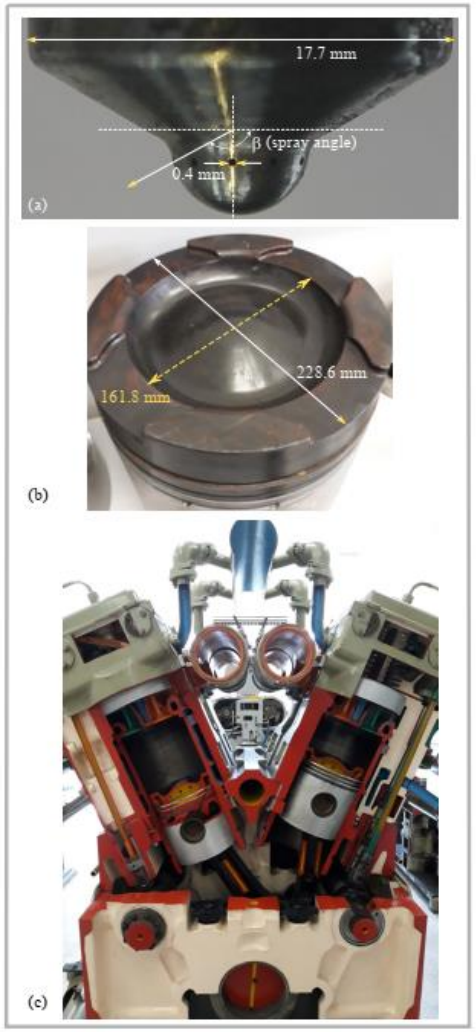

Figure 2: (a) Injector head magnification with main dimensions as input geometrical parameters. (b) Piston head, and (c) Picture of the locomotive GE 7FDL / DASH9-BB40W engine at VALE S.A.

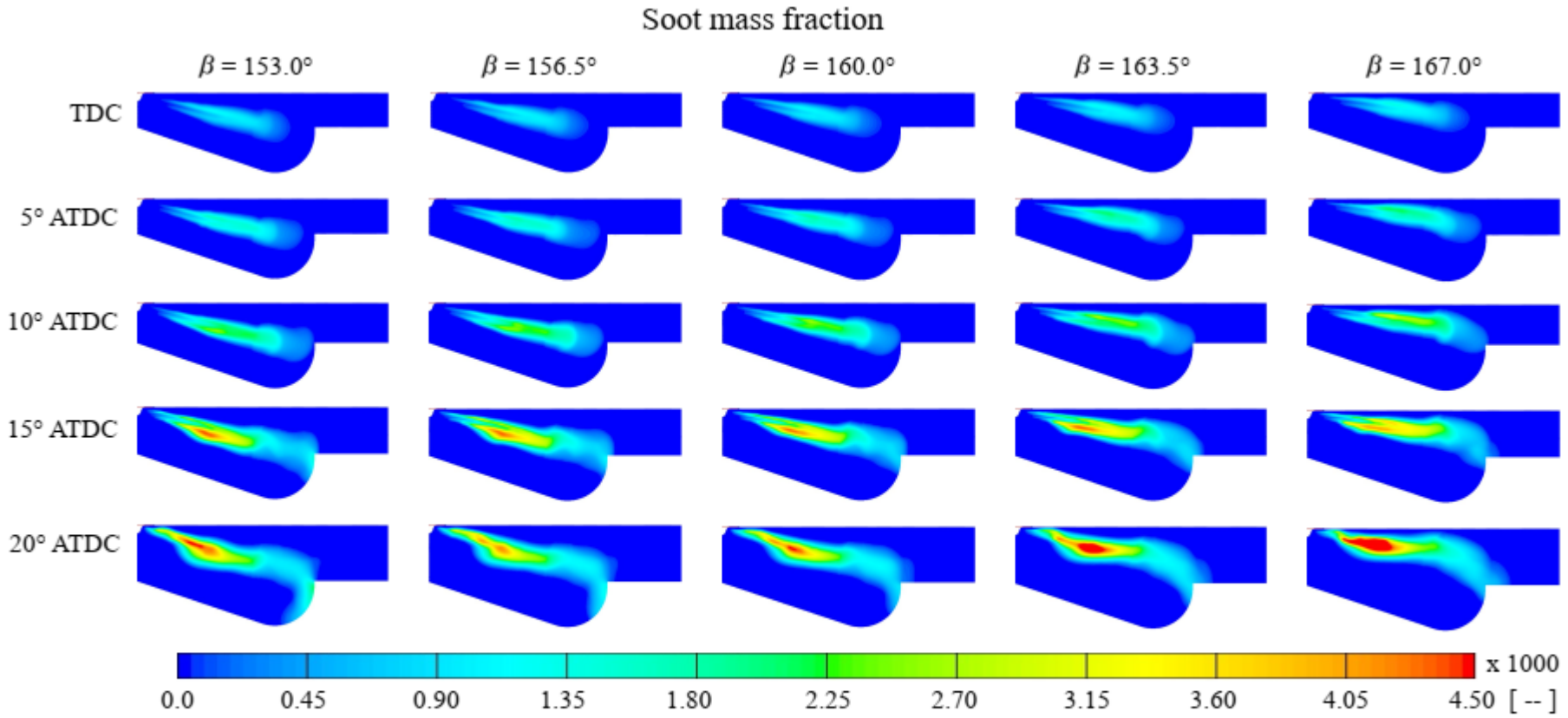

Figure 10: Soot mass fraction fields for all the spray angles (β) investigated in this work, along the first 20° crank angle after top dead center ($\Delta CA = 5^\circ$), at default engine injection timing (702 CA).